L-selectin regulates human neutrophil transendothelial migration

[1]Izajur Rahman, [2]Aida Collado Sánchez, [1]Jessica Davies, [1]Karolina Rzeniewicz, [1]Sarah Abukscem, [1]Justin Joachim, [1]Hannah Louise Hoskins Green, [1]David Killock, [2]Maria Jesus Sanz, [3]Guillaume Charras, [4]Maddy Parsons, [1]Aleksandar Ivetic*

[1]BHF Centre for Research Excellence, School of Cardiovascular Medicine and Sciences, King's College London, James Black Centre, 125 Coldharbour Lane, London SE5 9NU. [2]Department of Pharmacology, Faculty of Medicine and Odontology, University of Valencia, Av. Blasco Ibáñez 15, 46010 Valencia, Spain. [3]London Centre for Nanotechnology, University College London, London, UK. [4]Randall Centre for Cell and Molecular Biophysics, King's College London, New Hunt's House, Guy's Campus, London SE1 1UL, UK.

* Corresponding Author aleksandar.ivetic@kcl.ac.uk

Key words
PECAM-1
Diapedesis
Transmigration
p38 MAPK
JNK

Summary statement
Neutrophil L-selectin co-clusters with PECAM-1 in cis during transendothelial migration (TEM). Clustering neutrophil PECAM-1 activates p38 MAPK and JNK to regulate L-selectin shedding, which in turn expedites TEM.

Abstract

The migration of circulating neutrophils towards damage/infected tissue is absolutely critical to the inflammatory response. L-selectin is a cell adhesion molecule abundantly expressed on circulating neutrophils. For over two decades, neutrophil L-selectin has been assigned the exclusive role of supporting tethering and rolling – the initial stages of the multi-step adhesion cascade. Here, we provide direct evidence for L-selectin contributing to neutrophil transendothelial migration (TEM). We show that L-selectin co-clusters with PECAM-1 - a well-characterised cell adhesion molecule involved in regulating neutrophil TEM. This co-clustering behaviour occurs specifically during TEM, which serves to augment ectodomain shedding of L-selectin and expedite the time taken for TEM (TTT) to complete. Blocking PECAM-1 signalling (through mutation of its cytoplasmic tail), PECAM-1-dependent adhesion, or L-selectin shedding, led to a significant delay in the TTT. Finally, we show that co-clustering of L-selectin with PECAM-1 occurs specifically across TNF-α- but not IL-1β-activated endothelial monolayers – implying unique adhesion interactomes forming in a cytokine-specific manner. To our knowledge, this is the first report to implicate a non-canonical role for L-selectin in regulating neutrophil TEM.

Introduction

The rapid recruitment of circulating neutrophils to inflamed postcapillary venules, and their subsequent transendothelial migration (TEM), is absolutely essential to the inflammatory response. The multi-step adhesion cascade embodies a paradigm that describes the increasingly adhesive steps leukocytes take with the underlying inflamed endothelium prior to their exit from the microcirculation. Recent advances in understanding how cell adhesion molecules arrange in *cis* is now building a more complex framework of molecular interactions that are triggered during the adhesion cascade. For example, in mice, P-selectin glycoprotein ligand-1 (PSGL-1) co-clusters in *cis* with L-selectin (CD62L) in lipid rafts during neutrophil rolling to subsequently activate LFA-1/αLβ2 integrin (Stadtmann et al., 2013) and transition slow rolling towards arrest. Whilst this mechanism may not be conserved in humans (Morikis et al., 2017; Pruenster et al., 2015), it nonetheless provides a plenary example of how individual cell adhesion molecules coalesce into unique "interactomes" to advance the multi-step adhesion cascade.

There is excellent *in vivo* and *in vitro* evidence to suggest that 70-90% of all neutrophil TEM events adopt a paracellular route, leaving approximately 10-30% of TEM events to proceed via non-junctional routes (Ley et al., 2007; Muller, 2011; Woodfin et al., 2011). During paracellular TEM, leukocytes must disrupt junctions of adjoining endothelial cells and, concomitantly, limit excessive oedema. Numerous cell adhesion molecules have been identified at adherens and tight junctions, collectively retaining barrier integrity to regulate the movement of cells and macromolecules under steady-state and inflammatory conditions. Examples include: Junctional Adhesion Molecule (JAM)-A, -B and -C; Platelet-Endothelial Cell Adhesion Molecule-1 (PECAM-1); CD99; Intercellular adhesion molecule-2 (ICAM-2), Vascular Endothelial (VE)-Cadherin, occludin, nectin and the claudins (Allport et al., 1997a; Bradfield et al., 2007; Devilard et al., 2013; Huang et al., 2006; Lou et al., 2007; Ludwig et al., 2005; Reijerkerk et al., 2006; Schenkel et al., 2006; Woodfin et al., 2009). Most adherens or tight junctions form homotypic interactions between apposing endothelial cells. Junctional disruption during TEM is facilitated in part by the presence of complementary molecules on the leukocyte surface. Therefore, cell adhesion molecules such as PECAM-1 are subject to hetero-cellular homotypic interactions (i.e. displacing endothelial-endothelial PECAM-1 interaction with endothelial-leukocyte PECAM-1 interaction) (Privratsky et al., 2011). Studies in PECAM-1 knockout mice reveal contributions to early stages of TEM (Woodfin et al., 2009).

Whilst signalling downstream of PECAM-1 engagement has been extensively characterised at the molecular level in both platelets and endothelial cells, little is known about signalling in human leukocytes. Using the U973 monocyte-like cell line, Florey *et al* revealed that two tyrosine residues within the immunoreceptor tyrosine-based inhibition motif (ITIM) are phosphorylated when PECAM-1 is clustered during TEM to drive the transmigratory process (Florey et al., 2010). Phosphorylation of PECAM-1 at ITIM tyrosines 663 and 686 leads to its translocation into lipid rafts, where it is dephosphorylated to inactivate signal transduction during this period of TEM (Florey et al., 2010). Function-blocking antibodies to PECAM-1 (e.g. HEC7 for human and Mec13.3 for mouse PECAM-1)

can impede primary neutrophil and monocyte transmigration in various *in vitro* and *in vivo* models (Christofidou-Solomidou et al., 1997; Muller et al., 1993). Interestingly, mouse knock-out models of PECAM-1 have exposed conflicting data that imply strain-restricted phenotypes (Schenkel et al., 2006). The mechanistic conservation of TEM between mice and humans is therefore still unclear, in part due to the disparity in readouts amongst experimental models (i.e. complete emigration through multiple venular barriers for mouse *in vivo* assays versus entry into the subendothelial space for human *in vitro* assays).

L-selectin is expressed on most circulating leukocytes and is best known for its role in mediating tethering and rolling (Ivetic, 2018; Ivetic et al., 2019). Recently, L-selectin has been shown to exist in the protruding pseudopods of transmigrating CD14-positive human monocytes. Moreover, the pool of L-selectin in transmigrating pseudopods is clustered before it is cleaved by ectodomain shedding – suggesting the potential for L-selectin-dependent signalling during TEM (prior to shedding). L-selectin can be clustered via two distinct mechanisms: 'outside-in' and 'inside-out', where the former is driven by classic binding to extracellular ligands and the latter is driven by intracellular signals that lead to actin remodelling and clustering of the L-selectin tails. The majority of our understanding of L-selectin clustering is derived from studies using monoclonal antibodies or extracellular ligands to drive outside-in clustering (reviewed extensively elsewhere (Ivetic et al., 2019)). In this study, we asked whether inside-out modes of L-selectin clustering could be influenced by other cell adhesion molecules involved in the adhesion cascade. Indeed, we discovered that clustering PECAM-1 promoted the subsequent clustering of L-selectin. Moreover, these receptors co-cluster in *cis* in both primary human monocytes and neutrophils. The relationship of co-clustering between PECAM-1 and L-selectin was found to be unidirectional and non-reciprocal – further suggesting that co-clustering of these molecules is context-specific (e.g. during TEM, when PECAM-1 is engaged and clustered, rather than rolling when L-selectin is engaged and transiently clustered). Fluorescence Lifetime Imaging Microscopy (FLIM) revealed that L-selectin-RFP/PECAM-1-GFP co-clustered within distances of less than 10 nm in differentiated HL-60 (dHL-60) cells actively engaged in TEM under flow conditions. Moreover, L-selectin/PECAM-1 co-clustering was only witnessed in cells crossing TNF-α-, but not IL-1β-, activated endothelial monolayers. Direct antibody-mediated clustering of PECAM-1 on neutrophils potentiated ectodomain shedding of L-selectin. Moreover, the kinases Akt, JNK and p38 MAPKδ were robustly activated following clustering of neutrophil-derived PECAM-1 - suggesting a contribution of these downstream effectors in regulating L-selectin shedding during TEM. Blocking L-selectin shedding with the small molecule inhibitor, TAPI-0, resulted in significantly slower neutrophil transmigration times across TNF-α but not IL-1-β-activated endothelial monolayers, implying that L-selectin shedding optimises neutrophil TEM in a cytokine-specific manner. Taken together, we suggest that neutrophil TEM across TNF-α-activated endothelial monolayers drives the co-clustering of PECAM-1 and L-selectin to potentiate its shedding and expedite the time taken for TEM (TTT). To our knowledge, this study provides the first evidence for the direct involvement of L-selectin in regulating neutrophil TEM.

Materials and methods

Reagents and antibodies

All reagents were purchased from Sigma Aldrich, unless otherwise stated. TNF protease inhibitor-0 (TAPI-0) was purchased from Santa Cruz Biotechnologies and dissolved in DMSO. Anti-L selectin antibody, DREG56 (mouse monoclonal IgG1 κ), or Alexa Fluor®647nm-conjugated DREG56, was purchased from Santa Cruz Biotechnologies (Catalogue # sc-18851). Anti-human PECAM-1 (HEC7, mouse monoclonal IgG2a, Thermo Fisher Scientific: Catalogue # MA3100) and IgG isotype controls were purchased from Thermo Fisher Scientific. Anti-human PECAM-1 (sheep polyclonal IgG) was purchased from R&D Systems (Catalogue #AF806-SP) and targets the extracellular domain of PECAM-1. HEC7 is a mouse IgG2a monoclonal antibody that specifically targets immunoglobulin domains 1 and 2 of human PECAM-1. LAM1-14 mouse monoclonal IgG1 is a non-function-blocking antibody for human L-selectin and was kindly provided by Thomas Tedder (Duke University, USA)(Spertini et al., 1991). DREG56 specifically targets the lectin domain of human L-selectin and is a function-blocking antibody. It is noteworthy to mention that both HEC7 and LAM1-14 are both mouse monoclonals and could therefore not be used for clustering and secondary antibody labelling for confocal microscopy (as in Figure 1C and D). Instead, sheep anti-human PECAM-1 antibody (R&D Systems) was used.

Human Umbilical Vein Endothelial cells (HUVEC)

Human umbilical vein endothelial cells (HUVEC) were purchased from Lonza and expanded in fibronectin-coated 75cm^2 flasks (10 μg/mL in PBS) in a 37°C/5% CO_2 incubator until passage 4. HUVEC were grown using Lonza EGM-2 growth media supplemented with human Epidermal Growth Factor (hEGF), Vascular Endothelial Growth Factor (VEGF), R3-Insulin-like Growth Factor (R3-IGF-1) and human Fibroblast Growth Factor-Beta (hFGF-b). HUVEC were detached from flasks using trypsin-EDTA under conditions of 37°C/5% CO_2 for 3-5 min.

Culture/differentiation conditions for THP-1 cells and HL-60 cells

THP-1 cells were purchased from ATCC and cultured as previously published (Newe et al., 2019; Rey-Gallardo et al., 2018; Rzeniewicz et al., 2015). HL-60 cells stably expressing CXCR2 were kindly provided by Prof Ann Richmond (Vanderbilt University, USA) (Sai et al., 2006) and tested for contamination, but not recently authenticated. Cells were grown in HL-60 media (RPMI, (Gibco); 10% FCS; 1% penicillin streptomycin (Gibco)) and kept to densities of 0.5×10^6 per mL. Differentiation of HL-60 cells (dHL-60) was performed by culturing HL-60 cells at a density of 1×10^6 cells per mL in 1.3% dimethyl sulfoxide (DMSO).

Fluorescence-Activated Cell Sorting (FACS)

Cell lines were sorted by dedicated support staff at the Flow Cytometry Facility located in the Clinical Research Centre at Guy's and St Thomas' NHS Foundation Trust and King's College London, 15th floor, Tower Wing, Guy's Hospital, Great Maze Pond, London, SE1 9RT.

Mutagenesis of PECAM-1 and L-selectin.

Human PECAM-1 cDNA amplified from pWPT lentiviral plasmid, with open reading frames (ORFs) of WT and Y663, 686F (YYFF) mutant PECAM-1 (kindly donated by Dr Oliver Florey, Babraham Institute, UK (Florey et al., 2010)) and subcloned into pHR'SIN-SEW lentiviral vector containing the ORF of green fluorescent protein (GFP) 3' to the multiple cloning site. The primers used to amplify PECAM-1 were engineered to contain AscI and KpnI restriction sites at the 5' and 3' ends, respectively:

PECAM-1 forward primer: 5'-GAGAGAGGCGCGCCATGCAGCCGAGGTGGG-3'
PECAM-1 reverse primer 5'-CTCTCTGGTACCAGTTCCATCAAGGGAGCC-3'.

Sanger sequencing by Source BioScience (Nottingham, UK) ensured correct insertion of the PECAM-1 cDNA, and that no unexpected mutations or frame shifts occurred during the subcloning procedure. PCR-based mutagenesis of PECAM-1 was conducted according to the manufacturer's instructions (Agilent Technologies). The primers used for the generation of PECAM-1 small nucleotide polymorphisms (SNPs) are listed below. Following mutagenesis, all constructs were fully sequenced to confirm mutations had been faithfully incorporated. PECAM-1 in either its WT form or containing the tyrosine to phenylalanine substitutions at positions 663 and 686 (YYFF) was mutated as described by Florey et al., and subcloned into lentiviral vectors (pHR'SIN-SEW, see below).

WT and mutant L-selectin open reading frames were subcloned into pHR'SIN-SEW lentiviral vectors as previously described (Rzeniewicz et al., 2015). The lentiviral backbone vectors were provided by Adrian Thrasher, Institute of Child Health, University College London, London, United Kingdom, which carried either enhanced GFP (hereafter referred to as GFP) or monomeric mCherry (hereafter referred to as RFP) as C-terminal tags for PECAM-1 and L-selectin, respectively.

Generation of HL-60 cell lines

HL-60 cells stably expressing CXCR2 (kind gift from Prof. Ann Richmond (Vanderbilt University, USA) (Sai et al., 2006)) were infected with lentiviral particles containing the pHR'SIN-SEW vector and open reading frames for: GFP, L-selectin-RFP or PECAM-1-GFP. More information on the lentiviral vectors used can be found in our previous reports (Burns et al., 2010; Rey-Gallardo et al., 2018; Rzeniewicz et al., 2015). All HL-60 cells were prepared to a density of 1 x 10^6 cells per mL and subsequently infected with a multiplicity of infection of (MOI) 10 for each viral particle. After infection, cells were propagated until sufficient numbers were obtained for cell sorting at the dedicated flow cytometry facility at the National Institute for Health Research (NIHR) Biomedical Research Centre (Guy's Hospital, London). Sorted cells were analysed by FACS to validate equal expression between cell lines, as shown in Fig. S1.

Antibody-mediated clustering (AMC) of L-selectin or PECAM-1

Freshly isolated neutrophils were labelled with 1 μg/mL of either DREG-56 (a mouse IgG1κ monoclonal antibody directed at the lectin domain of human L-selectin), HEC7 (mouse IgG2a monoclonal antibody targeting immunoglobulin domains 1 and 2 of human PECAM-1), or anti-human PECAM-1 antibody (sheep polyclonal IgG) for 30 min on ice. It is noteworthy to mention that both HEC7 and LAM1-14 are both mouse monoclonals and could therefore not be used for clustering and secondary antibody labelling for confocal microscopy (as in Figure

1). Instead, sheep anti-human PECAM-1 antibody (R&D Systems) was used. All labelling procedures were conducted in Fc-receptor block (Miltenyi Biotec) and 33.3% foetal calf serum to ensure primary or secondary antibodies were not targeting the Fc-receptors. Labelling steps were followed by two wash steps in phosphate buffered saline to remove any excess antibody. Subsequent labelling with 10 μg/mL of either anti-mouse or anti-sheep secondary antibody conjugated to either Alexa Fluor®488 or 633 was used for microscopy post-fixation and overnight staining or FACS. After washing off excess secondary antibody, cells were resuspended in neat RPMI and then plated onto poly-L-lysine-coated coverslips for indicated timepoints. Cells were fixed in 4% paraformaldehyde (PFA) v/v in PBS without Ca^{2+} and Mg^{2+}. Specimens were further prepared for confocal, FRET/FLIM or inverted structural illumination microscopy (iSIM). Clustering experiments were performed at 37°C for 25 min.

Isolation of primary human neutrophils and CD14-positive monocytes
Primary human neutrophils were isolated from whole blood of healthy volunteers at the King's College Hospital Clinical Research Facility, in accordance with approval by the local research ethics committee at King's College London.
Freshly drawn blood (25 mL) was layered onto 15 mL of Histopaque-1077 and centrifuged at 186 g for 30 min at room temperature and pressure (RTP) with acceleration/deceleration set to 1/1, respectively. Three layers above a bottom layer of red blood cells formed after centrifugation: a yellow plasma layer; a buffy coat layer; and a clear Histopaque-1077 layer. The buffy coat was retained specifically for further isolation of CD14-positive monocytes, according to manufacturer's instructions (CD14 negative selection kit – Miltenyi Biotec), which we have published before (Rey-Gallardo et al., 2018; Rzeniewicz et al., 2015). We have previously published the isolation of neutrophils from whole blood in great detail (Killock and Ivetic, 2010).

MAPK array of primary human neutrophils following PECAM-1 clustering
A Proteome Profiler™ Human Phospho-MAPK Array Kit (R&D Systems) was used to assess which family of MAPKs became phosphorylated (and therefore activated) in response to PECAM-1 clustering. Ten million freshly isolated primary human neutrophils were left untreated or incubated with 1 μg/mL mouse anti-CD31 HEC7 on ice for 30 min in the presence of Fc Receptor block and 33% FCS, followed by clustering with a secondary anti-mouse antibody (see exact details in section above entitled: Antibody-mediated clustering (AMC) of L-selectin and PECAM-1). Neutrophils were subsequently harvested by centrifugation, excess antibody within the supernatant aspirated, and the pellet lysed with a proprietary lysis buffer. Following centrifugation at 13,000 g for 15 min to clarify the lysate, samples were incubated with the membrane-immobilised antibody array in accordance with the manufacturer's protocol. Membranes were left overnight at 4°C to incubate with gentle agitation. The following day, membranes were washed in PBS, blocked and probed (all at RTP) with a cocktail of biotinylated phospho-specific antibodies. Membranes were washed prior to incubation with streptavidin-horseradish peroxidase and a chemiluminescent reagent mix, before development by exposure to X-ray film. Images of the array were acquired by scanning the X-ray films and visualisation achieved using a GS-800 BioRad gel scanner.

Parallel plate flow chamber assays

All flow assays were conducted using the Glycotech platform. The experimental setup has been published in previous reports from our lab (Newe et al., 2019; Rey-Gallardo et al., 2018; Rzeniewicz et al., 2015). Importantly, HUVEC were grown to confluence of 35 mm circular coverslips (thickness = 1.0; purchased from Menzel Glaser, VWR), pre-coated with 10 µg/mL bovine fibronectin (diluted in PBS) and stimulated overnight (18h) with either 10 ng/mL recombinant human TNF-alpha (TNF-α, R&D Systems) or 10 ng/mL recombinant human interleukin-1 beta (IL-1β, Sino Biological®). All flow assays were performed at 1.5 dynes/cm^2. Cells exposed to the sheddase inhibitor, TAPI-0, or the p38 MAPK inhibitor, SB202190, were preincubated for 20 min prior to flow assays. Both TAPI-0 and SB202190 are reversible inhibitors, so leukocytes were exposed to the inhibitor beforehand, and the perfusate was also supplemented in the media (10 µM for TAPI-0 and 25 µM for SB202190). HUVEC were exposed to TAPI-0 but not SB202190 prior to flow chamber assays to limit the impact of the inhibitor specifically towards leukocytes and not endothelial cells. Control experiments were performed with the carrier, DMSO, as previously described (Rzeniewicz et al., 2015).

An Olympus IX81 epifluorescence microscope was used for all acquisitions of live flow assays, using the same bright field (for phase contrast) and fluorescence intensity settings (for GFP and RFP). A 10x objective lens was used (numerical aperture = 0.3^) for all acquisitions. All experiments were conducted under stable thermal setting of 37°C, by virtue of a bespoke heated chamber surrounding the microscope stage. Volocity software was used to control image acquisitions, taken by a Hamamatsu C10600 ORCA-R2 digital camera. Each frame was taken every 4 seconds for primary human neutrophils (phase only) and every 50 seconds for dHL60 cells (phase and fluorescence).

In assays where confocal microscopy or FRET/FLIM analysis is used, specimens were fixed immediately in 4% PFA and prepared for each respective technique as previously described (Newe et al., 2019; Rey-Gallardo et al., 2018; Rzeniewicz et al., 2015).

Calculating the time taken for transendothelial migration (TTT)

Imaging of transmigrating cells was performed using timelapse epifluorescence microscopy – where HL-60 cells would be serially imaged in phase and then fluorescence channels (to detect either PECAM-1-GFP or L-selectin-RFP). Images were acquired once every 4 seconds for primary human neutrophils (phase only) and every 50 seconds for dHL60 cells (phase and fluorescence). Using the phase channel, cells were tracked from the moment of adhesion to HUVEC from flow to the moment they have undergone full transendothelial migration. The transition from adhesion to complete TEM was scored as the change from being "phase bright" to "phase dark" - as shown in the stills 2-10 represented in Fig. 5A and Movies 2 and 3 for primary human neutrophils and dHL-60 cells, respectively.

Ectodomain shedding assays using flow cytometry and confocal microscopy

Primary human neutrophils were left untreated or incubated with HEC7 monoclonal antibody at 1 µg/mL for 30mins in blocking buffer (containing human Fc Receptor block (Miltenyi Biotec) and 33.3% foetal calf serum (FCS) in PBS) at 37°C. Excess (unbound) HEC7 antibody was subsequently washed by

centrifugation and resuspension of the pellet with RPMI-1640 media containing Fc receptor block and FCS. Clustering PECAM-1 in a subset of cells was performed by labelling cells on ice with Alexa Fluor®488 donkey anti-mouse antibody at 10 µg/mL for 5 or 30 mins at 37ᵒC to drive L-selectin clustering. After washing off excess secondary antibody in HL-60 media and blocking agents at room temperature, neutrophils were incubated in HL-60 media containing phorbol-12'-myristate-13'-acetate (PMA) at various concentrations, for 30mins at 37ᵒC. Neutrophils were then immediately transferred to ice-cold HL-60 media prior to washing steps and labelling with DREG56 directly conjugated to Alexa Fluor®647 for 30mins, at 4ᵒC. Neutrophils labelled with just HEC7 were also subsequently labelled with DREG56 conjugated to Alexa Fluor®647 for 30mins at 4ᵒC. In some experiments, neutrophils were preincubated for 10mins with either 10 µM TAPI-0 or 25 µM SB202190 at 37ᵒC prior to secondary antibody labelling. In each case, the inhibitor remained present during incubation with secondary antibody. Cells not challenged with secondary antibody or drugs were taken through the same procedure containing just carrier (DMSO) and/or non-specific isotype-matched antibody.

For monitoring L-selectin shedding induced by TEM (as in Figure 3), neutrophils were prepared for parallel plate flow chamber assays as described above. After 20 min of perfusion, specimens were rapidly fixed in 4% PFA and subsequently prepared for immunostaining. Specimens were washed three times in PBS and blocked using human Fc Receptor block (Miltenyi Biotec) and 33.3% foetal calf serum in PBS. The anti-L-selectin monoclonal antibody, LAM1-14, was used to detect L-selectin expression in neutrophils that had exclusively entered the subendothelial space (as shown in Fig. 5D&E).

Following 20 min of perfusion, under wide field microscopy, approximately 95% of all neutrophils had fully transmigrated and adopted a flat phase dark phenotype (see Movie 2). LAM1-14-positive staining of fully transmigrated neutrophils was assessed using the line intensity tool in Volocity software. Two diametrically opposed lines of equal length were created to bisect each cell that was under analysis (see Fig. 3C). The pixel intensity values of the 2 lines were averaged, and these mean intensity values were subsequently collected for every cell analysed. The total of fluorescence intensity values was then divided by the number of cells analysed across 3 independent experiments (i.e. ≤420 neutrophils per treatment group). The fluorescence intensity values for TAPI-0 treatment were normalised to represent maximal (100%) retention of L-selectin expression after TEM. This value was then used to determine the percentage loss of L-selectin expression in the DMSO treatment group.

Inverted structural illumination microscopy (iSIM)

Images were acquired at 100X magnification (1.49NA) on a vt-iSIM (a high-speed super resolution imaging system) with Hamamatsu Flash4.0 sCMOS camera and operated by Nikon NIS elements software. The vt-iSIM lasers used were at wavelengths: 488nm and 642nm. Z-stacks in 3D were obtained at a resolution of 0.12µm. Post-acquisition analysis involved deconvolution, which was performed in NIS elements, and applying the Richardson-Lucy algorithm at a mounting medium refractive index of 1.372. NIS elements software was used to obtain Mander's overlap coefficiencies (M2 Coeff) of L-selectin and PECAM-1 signal overlap by thresholding signals to eliminate background. Coefficients were

obtained for three distinct optical slices representing the apex (top), middle and base of primary human neutrophils.

Confocal microscopy and Mander's Overlap coefficiencies obtained by Volocity

Images of THP-1 cells and primary human monocytes were acquired using a Leica TCS SP5 microscope and a Leica oil immersion 63X objective lens (NA 1.4). Optical sections were acquired at a resolution of 0.72 μm. Images acquired by confocal microscopy were analysed by Volocity software to obtain Manders Overlap Coefficiency. Signal intensities were set above background for both green and blue channels, which respectively corresponded to PECAM-1 and L-selectin, using the voxel spy tool. Instrument parameter settings were maintained in all of the image acquisitions. Complete (100%) overlap between signals is designated as having a value of 1. All neutrophil images were acquired structured illumiation microscopy (see iSIM section). M2 Coeff were acquired using NIS elements software.

Western blotting of PECAM-1 from HUVEC monolayers

Confluent monolayers of HUVEC in 6-well plates were stimulated for 17 hours with 10ng/ml TNF-α, IL1-β, or no stimulation. Cells were subsequently lysed in 100μl 2x protein loading buffer supplemented with 200mM DTT and 100 units/ml benzonase nuclease before boiling at 100°C for 5 minutes. HUVEC lysates were loaded 25μl per sample into a NuPage 4-12% bis tris gel. Proteins were separated by SDS-PAGE using 1x NuPAGE MES SDS running buffer for 1 hour at 150v. Proteins were transferred to a nitrocellulose membrane, using XCell II Blot Module (Thermo Fisher Scientific), over 2.5 hours at 30v. Membranes were blocked for 1 hour in 5% milk powder in tris-buffered saline (TBS) before incubation with primary antibodies: sheep anti-human CD31 (1:200 dilution, R&D systems AF806) and mouse anti-human β-actin (1:4200 dilution) at 4°C overnight. Membranes were washed 3 times for 5 minutes in TBS and 0.1% (v/v) Tween-20 (TBST) followed by incubation with secondary antibodies: donkey anti-goat (1:15000, LiCOR IRDye® 680CW) or donkey anti-mouse (1:15000, LiCOR IRDye® 800CW) for 1 hour at room temperature. TBST washes were repeated, followed by a final wash with TBS for 5 minutes. Western blots were developed using the Odyssey CLx Near-Infrared Fluorescence Imaging System and Image Studio software was used to quantify relative band intensities.

Fluorescence resonance energy transfer and fluorescence lifetime imaging microscopy (FRET/FLIM)

dHL-60 cells stably expressing L-selectin-RFP and PECAM-1-GFP (either WT or mutant forms) were perfused over cytokine-activated (either IL-1β or TNF-α) HUVEC monolayers and fixed at the point that the majority of cells were captured in mid-TEM. Specimens were counterstained with anti-PECAM-1 antibody to determine the position of endothelial cell junctions. An example of a leukocyte captured in mid-TEM is provided in Figure 3A – where junctional staining of PECAM-1 is breached and where regions of the transmigrating cell are above and below the endothelium. Given that the enrichment of PECAM-1 is at cell-to-cell junctions, FRET was measured and quantified exclusively at breached junctions and readings were taken neither exclusively above (adherent and non-transmigrated) nor exclusively below (fully completed TEM) the endothelium.

FLIM measurement of FRET was performed with a multiphoton microscope system as described previously (Newe et al., 2019; Rey-Gallardo et al., 2018; Rzeniewicz et al., 2015). A Nikon TE2000E inverted microscope, combined with an in-house scanner and Chameleon Ti:Sapphire ultrafast pulsed multiphoton laser (Coherent Inc.), was used for excitation of GFP (at 890 nm). Fluorescence lifetime imaging capability was provided by time-correlated, single-photon counting electronics (SPC 700; Becker & Hickl). A 40× objective (NA 1.3) was used throughout (CFI60 Plan Fluor; Nikon), and data were acquired at 500±20 nm through a bandpass filter (35-5040; Coherent Inc.). Acquisition times of ~300 s at low excitation power were used to achieve sufficient photon statistics for fitting; avoiding either pulse pile-up or significant photobleaching. Data were analysed as previously described (Parsons et al., 2008). The FRET efficiency is related to the molecular separation of donor and acceptor and the fluorescence lifetime of the interacting fraction by:

$$\eta FRET = (R0^6/(R0^6 + r^6)) = 1 - \tau FRET/\tau d,$$

where $\eta FRET$ is the FRET efficiency, R0 is the Förster radius, r is the molecular separation, $\tau FRET$ is the lifetime of the interacting fraction and τd is the lifetime of the donor in the absence of an acceptor. The donor-only control is used as the reference against which all of the other lifetimes are calculated in each experiment. $\tau FRET$ and τd can also be taken to be the lifetime of the interacting fraction and non-interacting fraction, respectively. Quantification of FRET was made from all pixels within each cell that was analysed. All image collection and data analysis were performed using TRI2 software (developed by Paul Barber, Gray Cancer Institute, London, UK).

Results

PECAM-1 clustering drives inside-out clustering of L-selectin
To understand if non-integrin cell adhesion molecules contribute to inside-out clustering of L-selectin, THP-1 cells were engineered to co-express WT L-selectin C-terminally tagged to green and red fluorescent protein (GFP/RFP). Primary antibodies targetting specific cell adhesion molecules (CD43, JAM-A, PECAM-1, CD44 and PSGL-1) were used, in combination with secondary antibody, to drive their clustering (see materials and methods for details). Using FLIM, we could quantify increases in FRET efficiency between the GFP and RFP tags that would in turn reflect L-selectin clustering. Antibody-mediated clustering of L-selectin with the monoclonal antibody, DREG56, promoted maximal FRET efficiency in THP-1 cells co-expressing L-selectin-GFP/RFP to approximately 12% (Figure 1A). In THP-1 cells, clustering of endogenous PSGL-1 had no influence on the clustering of L-selectin-GFP/RFP, which is in agreement with a recent report by Morikis et al (Morikis et al., 2017). We however noticed that antibody-mediated clustering of either CD43 or PECAM-1 significantly increased the FRET efficiency of the L-selectin-GFP/RFP tags in THP-1 cells to 7% and 8% respectively (Figure 1A). Given that monocyte and neutrophil PECAM-1 have a well-established role in TEM (Muller et al., 1993; Thompson et al., 2001), and to determine if L-selectin plays a direct role in regulating TEM, we focused exclusively on the relationship between

L-selectin and PECAM-1. Moreover, studying the contribution of PECAM-1 to driving the co-clustering of L-selectin aligned with our recent interests in understanding how L-selectin contributes to monocyte protrusive behaviour in TEM (Newe et al., 2019; Rey-Gallardo et al., 2018; Rzeniewicz et al., 2015). To further determine if antibody-mediated clustering of PECAM-1 caused L-selectin to cluster locally or distally to PECAM-1 clusters, laser scanning confocal microscopy was used to quantify the extent of overlap in fluorescence signals corresponding to PECAM-1 and L-selectin. Manders Overlap Coefficiency (M2 Coeff) revealed that the extent of co-clustering between L-selectin and PECAM-1 increased significantly following antibody-mediated clustering of PECAM-1 (Figure 1B). Reciprocal experiments involving antibody-mediated clustering of L-selectin did not lead to the corresponding co-clustering of PECAM-1 (Figure 1B), implying a unidirectional relationship in co-clustering behaviour. The co-clustering of L-selectin with clusters of PECAM-1 could be recapitulated in both primary human monocytes (Figure 1C) and neutrophils (Figure 1D and movie 1). Whilst the majority of L-selectin/PECAM-1 clusters were present on the plasma membrane of primary neutrophils, a small amount localised to intracellular compartments (such as vesicles), suggestive of receptor internalisation (movie 1). Quantification by flow cytometry of neutrophil L-selectin confirmed that surface L-selectin expression decreased by 3.85% when just anti-PECAM-1 antibody was used, which increased to 22% upon crosslinking with secondary antibody (Figure 1E and Fig. S1&S2).

Co-clustering of L-selectin with PECAM-1 during TEM is cytokine-specific

Many *in vitro* transmigration assays have employed HUVEC monolayers stimulated with either TNF-α or IL-1β, with the broad assumption that the molecular mechanism guiding human neutrophil TEM is similar. Based on previous work in mice, where a cytokine-specific role for PECAM-1-dependent migration through venular walls has been documented (Thompson et al., 2001), we were motivated to explore whether the cytokines TNF-α or IL-1β could play divergent roles in driving the co-clustering of L-selectin with PECAM-1 - specifically during TEM. We have successfully used THP-1 cells to investigate mechanisms regulating L-selectin clustering in TEM, and its interaction with calmodulin or ERM proteins during TEM (Newe et al., 2019; Rey-Gallardo et al., 2018; Rzeniewicz et al., 2015). Due to their size, the majority of THP-1 cells are trapped in mid-TEM and rarely complete TEM (i.e. < 1% of all THP-1 cells undergo full TEM). Whilst this cellular model captures a high degree of cells in mid-TEM, so that the spatio-temporal organisation of interaction between L-selectin and binding partners can be closely interrogated, it precludes quantification of TEM to completion. In contrast, the neutrophil-like HL-60 cell line is smaller in size than THP-1 cells. However, they rarely transmigrate across activated endothelial monolayers. We noticed that stable expression of the chemokine receptor, CXCR2, dramatically improves TEM efficiency to approximately 80% (see Fig. S2). This observation has been recently reported by others (Yadav et al., 2018) and clearly reveals the essential role of CXCR2 in driving TEM of HL-60 cells. Both L-selectin and PECAM-1 are poorly expressed in HL-60 cells, which allowed us to develop a cellular model to interrogate their respective contribution to TEM (see Fig. S3 and S4). Using this cell line, we could test if the stable expression of L-selectin-RFP and PECAM-1-GFP would drive their co-clustering specifically during TEM.

HL-60 cells stably expressing L-selectin-RFP and PECAM-1-GFP were seeded onto poly-L-lysine (PLL)-coated coverslips to monitor the extent of FRET between the GFP and RFP tags using FLIM. Negligible co-clustering between PECAM-1-GFP and L-selectin-RFP was witnessed within a sub-10 nm resolution (0.982% ± 0.111, Figure 2A, upper row). This cell line was subsequently differentiated using 1.3% DMSO (hereon termed dHL-60 cells – see materials and methods for further details) and perfused over activated endothelial monolayers to assess co-clustering by FRET. Indeed, a 5-fold increase in FRET efficiency between the GFP/RFP tags (5.392% ± 0.338) was observed when cells were perfused over TNF-α-activated HUVEC (Figure 2A, middle row and Figure 2B). In contrast, perfusion of the same stable cell line over IL-1β-activated HUVEC led to negligible changes in FRET efficiency compared to cells adhering to PLL (1.208% ± 0.142, Figure 2A lower row and Figure 2B).

L-selectin shedding is triggered in transmigrating neutrophils in a cytokine-specific manner

The TEM of neutrophils across activated HUVEC is known to drive ectodomain shedding of L-selectin via a disintegrin and metalloproteinase (ADAM)17 sheddase activity (Allport et al., 1997b; Smith et al., 1991). Flow cytometric analysis of L-selectin on fully transmigrated neutrophils, retrieved after subjection to static TEM assays (i.e. in the absence of shear stress), revealed that they are predominantly L-selectin-negative (Allport et al., 1997b). To monitor the extent of L-selectin shedding from primary human neutrophils transmigrating into the subendothelial space of TNF-α- or IL1-β-activated HUVEC monolayers, cells were perfused for 20 min and immediately fixed in 4% paraformaldehyde (PFA). Specimens were subsequently permeabilised and stained for L-selectin using the LAM1-14 monoclonal antibody (Spertini et al., 1991), followed by detection with fluorescently-conjugated secondary antibody. Neutrophils captured in mid-TEM retained expression of L-selectin in both pseudopods and uropods (Figure 3A) – consistent with what has been documented in CD14+ human monocytes (Rzeniewicz et al., 2015). Of note, PECAM-1 protein expression did not change between untreated (UNT) or cytokine-activated endothelial monolayers (Figure 3B). To better interrogate the extent of L-selectin shedding in fully transmigrated neutrophils, similar experiments were conducted with 10 μM TNF-α protease inhibitor (TAPI-0) supplemented into the perfusate (see materials and methods for more detail). Direct comparisons in the percentage change of LAM1-14 fluorescence intensities were quantified between neutrophils crossing TNF-α− or IL1-β-activated HUVEC – with and without TAPI-0 (see Materials and Methods for more detail and Figure 3C). Neutrophils within the subendothelial space of TNF-α-activated HUVEC monolayers retained 67.53% (± 6.5%) of the LAM1-14 fluorescence signal compared to TAPI-0-treated neutrophils (Figure 3D). These observations imply ectodomain shedding is triggered, but not as robustly as previously reported in other indirect methods. In contrast, no significant reduction in LAM1-14 fluorescence was observed in neutrophils crossing IL-1β-activated HUVEC (Figure 3E). Taken together, these data demonstrate cytokine-specific effects on L-selectin shedding in neutrophils that have entered the subendothelial space. These results further show that L-selectin is turned over differently between neutrophils and CD14+ monocytes,

where the extent of L-selectin shedding in monocytes appears to be much higher (Rzeniewicz et al., 2015).

Antibody-mediated clustering of PECAM-1 sensitises L-selectin shedding in primary human neutrophils

We and others have previously shown that L-selectin shedding can be activated by the involvement of PKC or p38 MAPK (Killock and Ivetic, 2010). Using a MAPK array, we could show that clustering of PECAM-1 could activate p38 MAPK δ and JNK (Figure 4A), suggesting that these kinases may have an influence in regulating L-selectin shedding. Phospho-Akt was also strongly activated in response to PECAM-1 clustering, which is in keeping with a previous finding that PECAM-1 can co-precipitate the p85 subunit of PI3K (Pellegatta et al., 1998). To further ascertain if PECAM-1 clustering during TEM could augment ectodomain shedding of L-selectin, we clustered PECAM-1 with the monoclonal antibody, HEC7, on freshly isolated neutrophils (to mimic homotypic ligation via Ig domains 1 and 2) – with and without further clustering with secondary monoclonal antibody. Cells were subsequently challenged with increasing concentrations of phorbol myristate acetate (PMA - a potent inducer of L-selectin shedding) to activate PKC. Neutrophils pretreated with HEC7 antibody did not influence PMA-induced shedding any differently to neutrophils labelled with control IgG (Figure 4B). In contrast, clustering HEC7 with secondary antibody dramatically sensitised PMA-induced shedding of L-selectin on neutrophils (Figure 4B). We next asked if p38 MAPK played a role in sensitising L-selectin shedding following clustering of PECAM-1. Preincubation of neutrophils with 25 μM of the p38 MAPK inhibitor, SB202190, reverted the L-selectin shedding profile to neutrophils treated with either control antibody or HEC7 antibody (Figure 4C). Interestingly, inhibition by SB202190 was only observed at 2 nM PMA. This result would suggest that increasing the concentration of PMA would override the inhibitory effect of SB202190. Taken together, our data suggest that L-selectin shedding is sensitised by PECAM-1 clustering and this mechanism likely involves p38 MAPK δ. Our attempts to assess blocking JNK activity in similar assays showed that the JNK inhibitor (JNKi) SP600125 was sufficient to promote L-selectin shedding without any prior clustering of PECAM-1 (Figure 4D). These data imply that both JNK and p38 MAPK may act in opposition to regulate ectodomain shedding when PECAM-1 is clustered during TEM.

Co-expression of L-selectin and PECAM-1 expedites TTT across TNF-α-, but not IL-1β-, activated HUVEC monolayers.

As L-selectin/PECAM-1 co-clustering occurred exclusively during TEM (Figure 2), we next sought to address whether this co-clustering impacted TTT. Compared to THP-1 cells, HL-60 cells express negligible PECAM-1 and L-selectin (see Fig. S3). Stable dHL-60 cell lines expressing GFP alone (control cell line), or single and double combinations of PECAM-1-GFP and L-selectin-RFP, were perfused over TNF-α or IL-1β-activated HUVEC and the time taken from initial capture to complete TEM was recorded and quantified for at least 180 cells (see Figure 5A and Movie 3 for visual representation of "phase bright" captured cells and "phase dark" fully transmigrated cells). dHL-60 cells expressing GFP alone (which acted as control cells for lentivirally transduced dHL-60 cells) possessed similar TEM times across either TNF-α- or IL-1β-activated HUVEC monolayers (i.e. 9 min 29

sec (± 20 sec) for TNF-α vs 9 min 9 sec (± 18 sec) for IL-1β). These TEM times were similar to dHL-60 cells expressing a single cell adhesion molecule and crossing TNF-α-activated HUVEC monolayers (L-selectin-RFP = 9 min 5 sec (± 16 sec); PECAM-1-GFP = 9 min 40 sec (± 22 sec)). In contrast, dHL-60 cells co-expressing L-selectin-RFP and PECAM-1-GFP displayed significantly reduced TTT - taking 6 min 28 sec (± 14 sec) to cross TNF-α-activated HUVEC monolayers (Figure 5B). Interestingly, dHL-60 cells expressing just PECAM-1-GFP expedited TTT across IL-1β-activated HUVEC monolayers in 6 min 43 sec (± 13 sec) - yet took 9 min 40 sec (± 22 sec) to cross TNF-α-activated monolayers (Figure 5C). These data strongly suggest that stable expression of PECAM-1-GFP is sufficient to drive the faster TTT phenotype across IL-1β-activated HUVEC monolayers (Figure 5C).

To further understand the importance of this mechanism in primary human neutrophils, we used HEC7 to selectively block neutrophil PECAM-1 and determine whether TEM was impacted in a cytokine-specific manner. HEC7 targets the first two N-terminal immunoglobulin (Ig) domains in PECAM-1, which are responsible for supporting homophilic interaction and clustering *in trans* (Paddock et al., 2016) (i.e. between adjoining endothelial cells). In agreement with the dHL-60 cellular model, HEC7 retarded the TTT for primary human neutrophils crossing TNF-α- but not IL-1β-stimulated HUVEC monolayers (from 2.6 min (± 3 sec) to 3.5 min (± 6 sec), Figure 5D&E). These data suggest the Ig domains 1 and 2 of neutrophil PECAM-1 are important to expedite human neutrophil TEM across TNF-α-, but not IL-1β-activated HUVEC monolayers.

Blocking ectodomain shedding of L-selectin reduces TTT across TNF-α–, but not IL-1β-, activated HUVEC.

To further explore the relationship between L-selectin co-clustering with PECAM-1 during TEM, L-selectin shedding and the TTT, we closely examined the time it took for primary human neutrophils to fully complete TEM across TNF-α-activated HUVEC monolayers in the presence or absence of TAPI-0. In the presence of carrier alone (DMSO), neutrophils would average TTT of 2.5 min (± 3 sec), which would decrease significantly to 3.7 min (± 7 sec) in the presence of TAPI-0 (Figure 6A). In contrast, perfusion of neutrophils over IL-1β-activated HUVEC monolayers led to averaged TTT of 2.6 min (± 2 sec) in the presence of DMSO carrier and 2.7 min (± 2 sec) in the presence of TAPI-0 (Figure 6B). These data strongly imply that L-selectin shedding is triggered during TEM across TNF-α-activated HUVEC to expedite TTT, which is not the case for neutrophils crossing IL-1β-activated HUVEC monolayers.

We next addressed whether the expression of a non-cleavable mutant of human L-selectin, called ΔM-N L-selectin (Chen et al., 1995), could phenocopy the reduction in TTT characterised in neutrophils (Figure 6A&B and see materials and methods for information on ΔM-N L-selectin). Perfusion of dHL-60 cells, stably expressing just WT L-selectin-RFP, over TNF-α-activated HUVEC possessed an average TTT of 9 min 5 sec (± 16 sec). This time was further delayed to 10 min 21 sec (± 18 sec) when TAPI-0 was supplemented into the perfusate (Figure 6C). Perfusion of dHL60 cells co-expressing L-selectin-RFP and PECAM-1-GFP, as shown before (Figure 5B), had TTT of 6 min 28 sec (± 14 sec), which reduced significantly to 9 min 51 sec (± 16 sec) when TAPI-0 was supplemented into the

perfusate (Figure 6C). Taken together, these results phenocopied the effect of using TAPI-0 on neutrophils crossing TNF-α-activated HUVEC monolayers.

dHL-60 cells stably co-expressing PECAM-1-GFP and ΔM-N L-selectin-RFP possessed TTT that were similar to TAPI-0-treated double expressors (expressing WT L-selectin and PECAM-1), with an average TTT of 9 min 18 sec ($\pm$ 15 sec) (Figure 6C). In keeping with blocking L-selectin shedding in neutrophils, the migration times were significantly slower when dHL-60 cells were perfused over IL-1β-activated endothelial monolayers (i.e. 7 min 25 sec ($\pm$ 12 sec) – see Figure 6D). Whilst the TTT was significantly slower, the difference was modest compared against TTT across TNF-α-activated HUVEC monolayers (compare Figures 6C & D). In Figure 4B, the p38MAPK inhibitor significantly blunted the influence of PECAM-1 clustering in augmenting L-selectin shedding at low doses of PMA stimulation. We therefore supplemented the perfusate with either DMSO or 25 μM SB202198 to determine if inhibition of p38MAPK would impact TTT of primary human neutrophils. Indeed, neutrophil TTT were significantly retarded across both TNF-α- and IL-1β- activated HUVEC monolayers (Figure 6E & F). However, these TTT could not be directly attributed to SB202198 specifically blocking L-selectin shedding.

The contribution of PECAM-1 ITIM in regulating co-clustering of L-selectin and TTT

The intracellular tails of L-selectin and PECAM-1 can both interact with ERM proteins (Gamulescu et al., 2003; Ivetic et al., 2002). With respect to L-selectin, ERM binding is absolutely fundamental to antibody-mediated (outside-in) clustering (Newe et al., 2019). PECAM-1 also harbours an immunoreceptor tyrosine-based inhibition motif (ITIM) within its relatively longer cytoplasmic domain. Previous work by Florey *et al* revealed that two ITIM tyrosine (Y) residues at position 663 and 686 were responsible for modulating TEM of monocyte-like U937 cells in vitro (Florey et al., 2010). Given the unidirectional influence of PECAM-1 on driving the co-clustering of L-selectin during TEM, we questioned if mutation of Y663 and Y868 to non-phosphorylatable phenylalanines (F) would impact the co-clustering of L-selectin and therefore retard the TTT. HL-60 cells were therefore engineered to stably express both WT L-selectin-RFP and PECAM-1-GFP containing the Y663F and Y686F mutations (hereon called YYFF). As with cells expressing WT forms of L-selectin and PECAM-1, seeding HL-60 cells co-expressing WT L-selectin-RFP and YYFF PECAM-1-GFP onto PLL led to negligible increases in FRET efficiency as assessed by FLIM (Figure 7A and B). FRET/FLIM analysis revealed no significant increases in FRET efficiency between the GFP/RFP tags pairs when these dHL-60 cell lines were perfused over either TNF-α- or IL-1β-activated HUVEC (Figure 7C-F). Perfusion of dHL-60 cells over cytokine-activated HUVEC revealed that TTT reduced significantly in YYFF cells compared to WT cells over TNF-α-stimulated HUVEC (i.e. 9 min 6 sec ($\pm$ 17 sec) for YYFF cells vs 6 min 28 sec ($\pm$ 14 sec) for WT cells) (Figure 7G). However, the TTT of YYFF cells crossing IL-1β-activated HUVEC monolayers did not differ significantly from dHL-60 cells expressing WT versions of PECAM-1-GFP and L-selectin-RFP (Figure 7H). These data indicate an absolute requirement of the PECAM-1 ITIM to regulate the co-clustering of L-selectin and TTT of dHL-60 cells crossing TNF-α-, but not IL-1β-, activated HUVEC monolayers.

Discussion

Many investigations have shown neutrophils to be the first immune cell subtype to arrive at a site of extravascular damage or infection. The biological advantage of rapidly deploying neutrophils is to expedite their effector functions and mitigate death to the host (Ley et al., 2018). Our data predicts that blocking L-selectin/PECAM-1 co-clustering in humans would lead to an approximate 30% reduction in TTT, which, in theory, could reduce the chance of host survival. Blocking L-selectin shedding in human neutrophils with TAPI-0-like compounds was shown not to interfere with TEM (Allport et al., 1997b). It now seems likely that this oversight was down to the lack of close imaging of migration. Beyond TEM, it appears that blocking L-selectin shedding impacts neutrophil chemotaxis in vivo (Venturi et al., 2003), suggesting that effector functions may be impaired. Indeed, blocking L-selectin shedding in vivo appears to impair bacterial killing in vivo (Cappenberg et al., 2019).

L-selectin clustering can be promoted in one of two ways: outside-in (e.g. by ligand) and inside-out, e.g. by virtue of an intracellular signal that drives ligand-independent clustering – likely through the reorganisation of the cortical actin-based cytoskeleton. A plenary example of inside-out clustering of L-selectin was demonstrated by exposing T lymphocytes to fever-range temperatures (i.e. 38–41°C), which in turn triggers IL-6-dependent signalling to drive MEK/ERK-mediated L-selectin/cytoskeleton interactions (Chen et al., 2004; Evans et al., 1999; Wang et al., 1998). Chimeric fusion of DNA gyrase to the cytoplasmic tail of L-selectin can promote dimerisation of L-selectin in response to coumermycin treatment (Li et al., 1998). In both these cases, inside-out clustering of L-selectin increases avidity and therefore adhesion to immobilised ligands under hydrodynamic shear stress. Indeed, Figure 1 clearly shows, in the absence of an L-selectin ligand, antibody-mediated clustering of PECAM-1 is sufficient to drive this co-clustering behaviour. Experimentally, we have shown in THP-1 monocytes that L-selectin clustering occurs in transmigrating pseudopods and not within the non-transmigrated uropods (Rey-Gallardo et al., 2018; Rzeniewicz et al., 2015). Our data here would suggest that the co-clustering of L-selectin with PECAM-1 could drive L-selectin into clusters, to increase its avidity for adhesion to other non-sialyl Lewis-x ligands (such as biglycan) within the subendothelial space (see Fig. 8). Heparan sulfate proteoglycans (HSPGs) are reportedly enriched in the basolateral aspect of the endothelium (Stoler-Barak et al., 2014). Furthermore, we and others have shown that the HSPGs biglycan and versican are credible ligands for L-selectin (Celie et al., 2009; Kawashima et al., 2000; Kawashima et al., 1999; Kitaya and Yasuo, 2009; Rzeniewicz et al., 2015). We believe that signals downstream of L-selectin/HSPG binding would be sustained, as the absence of shear stress in the subendothelial space cannot break the L-selectin/HSPG bonds. The signals propagated in this region would therefore lead to as yet unidentified signals driving pseudopod protrusion in TEM. L-selectin-dependent signalling is potentially self-limiting, as clustering of L-selectin on neutrophils is sufficient to drive its ectodomain shedding (Palecanda et al., 1992).

Our hypothetical model of how PECAM-1 and L-selectin corroborate to drive pseudopod protrusion in TEM is summarised in Fig. 8. Whilst we know that monocyte-derived (U937 cell) PECAM-1 enters lipid rafts during TEM (Florey et

al., 2010), we speculate that L-selectin and PECAM-1 may co-cluster specifically within lipid rafts during TEM. Within this microdomain, it is possible that the exchange of ezrin for moesin on L-selectin can occur. We have shown that serine phosphorylation of the L-selectin tail at position S364 can abrogate ERM binding in vitro (Newe et al., 2019). And that clustering of L-selectin in Jurkat T-cells can drive cytoplasmic tail phosphorylation and subsequent enrichment into lipid rafts (Phong et al., 2003). These independent observations would imply that the transient and sequential phosphorylation of L-selectin and PECAM-1 cytoplasmic tails could drive their accumulation into lipid rafts - wherein ERM exchange could ensue. We also noticed that antibody-mediated clustering of PECAM-1 led to a 22% reduction in L-selectin expression, likely through internalisation and not shedding. Currently, we are not sure if this is a caveat to the experimental procedure, or if internalisation of L-selectin occurs during TEM.

Akt - a faithful biochemical readout for PI3K activation – was robustly activated following PECAM-1 clustering. An early observation showed that PECAM-1 can associate (directly or indirectly) with the p85 regulatory subunit of PI3K (Pellegatta et al., 1998). Whether co-clustering of L-selectin with PECAM-1 is required for PI3K activation is yet to be tested. We also observed an increase in phospho-JNK following PECAM-1 clustering (Fig. 4A). SP600125-mediated shedding of L-selectin in neutrophils suggests that JNK may be constitutively active to protect L-selectin from shedding when PECAM-1 is clustered. Activation of JNK would therefore be in conflict with synchronous activation of p38 MAPK, which primes L-selectin for shedding (Killock and Ivetic, 2010). It is tempting to speculate that JNK activation could be transient, whereas activation of p38 MAPK is more sustained. Therefore, protection of L-selectin shedding (through JNK activation) in early TEM could protect signals downstream of L-selectin that are necessary for pseudopod protrusion. Upon JNK inactivation (e.g. when neutrophils begin to enter the subendothelial space), p38 MAPK activity may then preside to prime L-selectin for ectodomain shedding in late TEM. L-selectin clustering in neutrophils can also prime neutrophil effector function (Smolen et al., 2000). Whether these effects of L-selectin are enhanced when PECAM-1 is clustered is yet to be determined.

Another compelling finding in this study is the cytokine-specific contribution of L-selectin/PECAM-1 co-clustering in regulating TTT specifically across TNF-α-, but not across IL-1β-, activated HUVEC monolayers. Our data imply that neither Ig domains 1&2 of neutrophil PECAM-1, nor the ITIM residues Y663 and Y686, are required for optimal TEM across IL-1β-activated HUVEC monolayers. Currently, it is not known if IL-1β can upregulate a unique (glyco)protein(s) to co-operate with PECAM-1 and alleviate the need for Y663 & Y686 and Ig domains 1 & 2 for optimised TEM. A comparative proteomic analysis of (glyco)protein expression in HUVEC, following stimulation with either IL-1β or TNF-α, could facilitate a better understanding of whether an additional factor may be involved in driving PECAM-1-dependent TEM across IL-1β-activated HUVEC. A recent report shows that neutrophils harvested from synovial fluid aspirates of patients with chronic inflammatory arthritis are L-selectin-positive (Bjorkman et al., 2018). In contrast, neutrophils harvested from acutely formed skin blisters are L-selectin-negative. Whether this observation implies neutrophils are crossing a higher proportion of

IL-1β-activated post-capillary venules in chronically inflamed joints (compared to post-capillary venules in acutely inflamed skin blister) would be an interesting topic to investigate further. If this is indeed the case, then quantifying the extent of L-selectin-positive neutrophils in a given histopathological section may act as a useful readout for the predominance of TNF-α or IL-1β within a given histopathological specimen.

N = 1
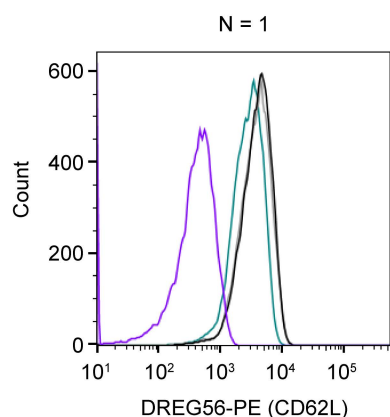
	Sample Name	Subset Name	Count	Median : FL2-A	Median : FL4-A
☐	C01 2Aug Cells Alone.fcs	Neutrophils	18180	400	244
☐	C02 2Aug Cells DREG56-PE.fcs	Neutrophils	18435	3928	243
☐	C04 2Aug HEC7 + D56-PE.fcs	Neutrophils	17964	3745	247
☐	C03 2Aug HEC7+2o 0`+D56-PE.fcs	Neutrophils	18502	2826	3854

N = 2
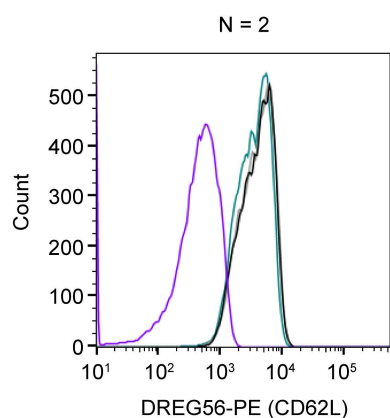
	Sample Name	Subset Name	Count	Median : FL2-A	Median : FL4-A
☐	A01 3 Ago Cells alone.fcs	Neutrophils	19083	453	261
☐	A02 3 Ago Cells D56-PE.fcs	Neutrophils	17969	4099	284
☐	A03 3 Ago HEC7+ D56-PE.fcs	Neutrophils	18184	4110	285
☐	A04 3 Ago HEC7+2o 0`+ D56-PE.fcs	Neutrophils	19053	3561	4780

N = 3
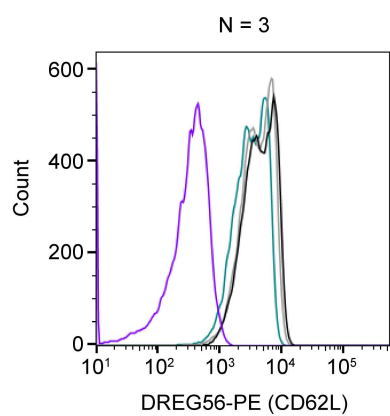
	Sample Name	Subset Name	Count	Median : FL2-A	Median : FL4-A
☐	G10 4Aug Cells Alone.fcs	Neutrophils	19335	330	217
☐	G11 4Aug Cells DREG56-PE.fcs	Neutrophils	19029	4380	223
☐	G12 4Aug HEC7+D56-PE.fcs	Neutrophils	19434	4066	226
☐	H01 4Aug HEC7+2o 0`+D56-PE.fcs	Neutrophils	19216	3185	3496

— Unlabelled

— HEC7 + DREG56-PE

— DREG56-PE

— HEC7 XL (Alexa Fluor® 647) + DREG56-PE

Supplementary Figure 1

Fig. S1

The effect of clustering PECAM-1 on surface L-selectin levels.

Flow cytometric analysis of primary human neutrophils treated with the anti-PECAM-1 monoclonal antibody, HEC7. Neutrophils were treated with HEC7 alone (grey line) or HEC7 plus a secondary clustering antibody conjugated to Alexa Fluor® 647 (green line). DREG56 directly conjugated to phycoerythrin was used to monitor L-selectin expression in untreated cells (black line), and cells with HEC7 alone (grey line) or with HEC7 plus clustering secondary antibody (green line). Purple line represents unstained neutrophils.

Percentage surface L-selectin levels, measured after HEC7 binding (with and without 2^{ary} mAb clustering)
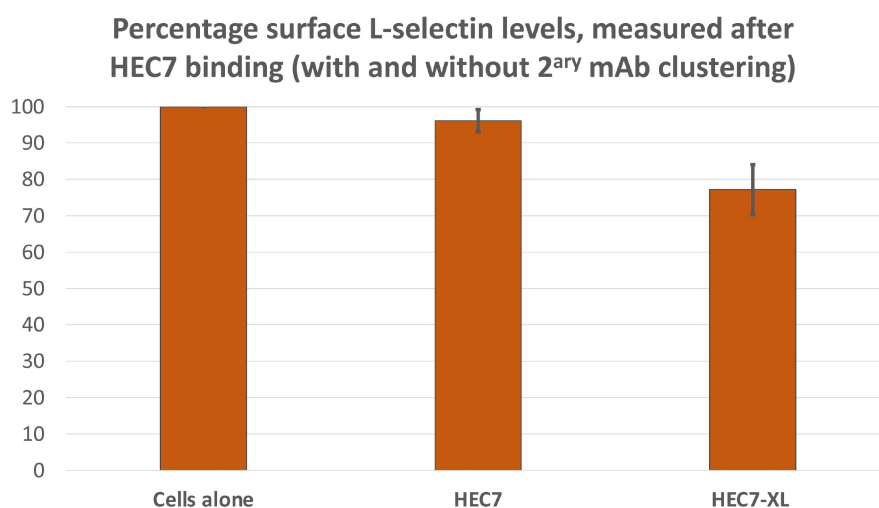
Supplementary Figure 2

Fig. S2
Summary of the data presented in Fig. S1
Bar graphs showing the impact of clustering PECAM-1 with HEC7 and secondary cross-linking monoclonal antibody can lead to a 22% reduction in L-selectin levels. Value of each bar: Cells alone = 100%; HEC7 = 96.15%; HEC7-XL = 77.18%
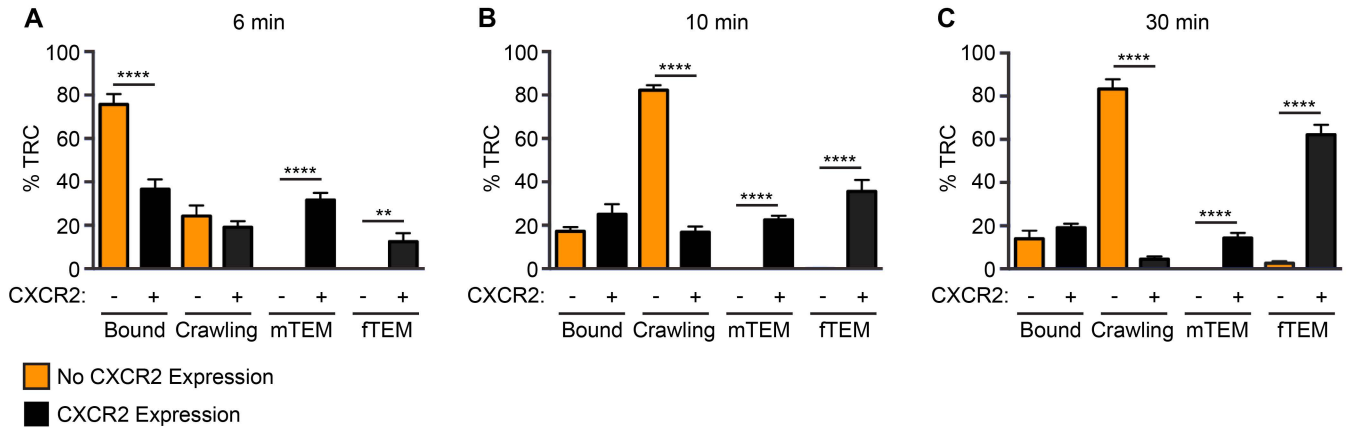
Supplementary Figure 3

Fig. S3
CXCR2 is essential for HL-60 TEM.
dHL-60 cells (orange bars) or dHL-60 cells stably expressing CXCR2 (black bars) were perfused over HUVEC monolayers, which were stimulated overnight with TNF-α. Flow assays were recorded as described in materials and methods (and see Movie 3 and stills in Fig. 5A). Transendothelial migration was scored by scoring for phase contrast. Cells were scored at 6 min, 15 min and 30 min. At each time point cells were scored as "Bound", "Crawling", in "mid-TEM" (see still images in panels 6 – 9 as an example of mid-TEM in Fig. 5A) or "full TEM" (see still image in panel 12 as an example of full TEM in Figure 5A). Error bars represent standard error of the mean. Statistical significance was assessed using an unpaired Student t-test, comparing the different cell lines at each separate stage of the adhesion cascade. **p<0.01, ***p<0.001 and ****p<0.0001.
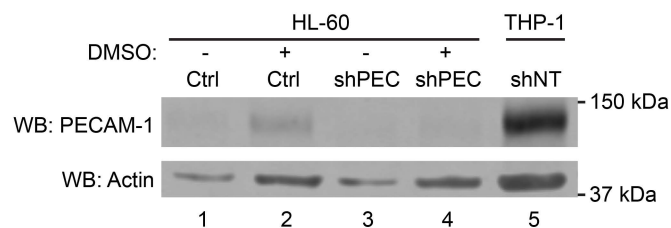
Supplementary Figure 4

Fig. S4

HL-60 cells express negligible levels of PECAM-1

Western blotting of whole cell lysates from THP-1 cells and HL-60 cells (stably expressing CXCR2) reveal that endogenous PECAM-1 is lowly expressed in HL-60 cells (lane 1), but highly expressed in THP-1 cells (lane 5). Low level PECAM-1 is expressed in HL-60 cells when differentiated in 1.3% DMSO (lane 2). This signal was deemed specific, as its expression could be reduced using lentiviral short hairpin (sh) RNA targeting PECAM-1. Given the low level of endogenous PECAM-1 in HL-60 cells, shRNA was not used to knock-down endogenous PECAM-1 in experiments requiring the expression of GFP-tagged PECAM-1.
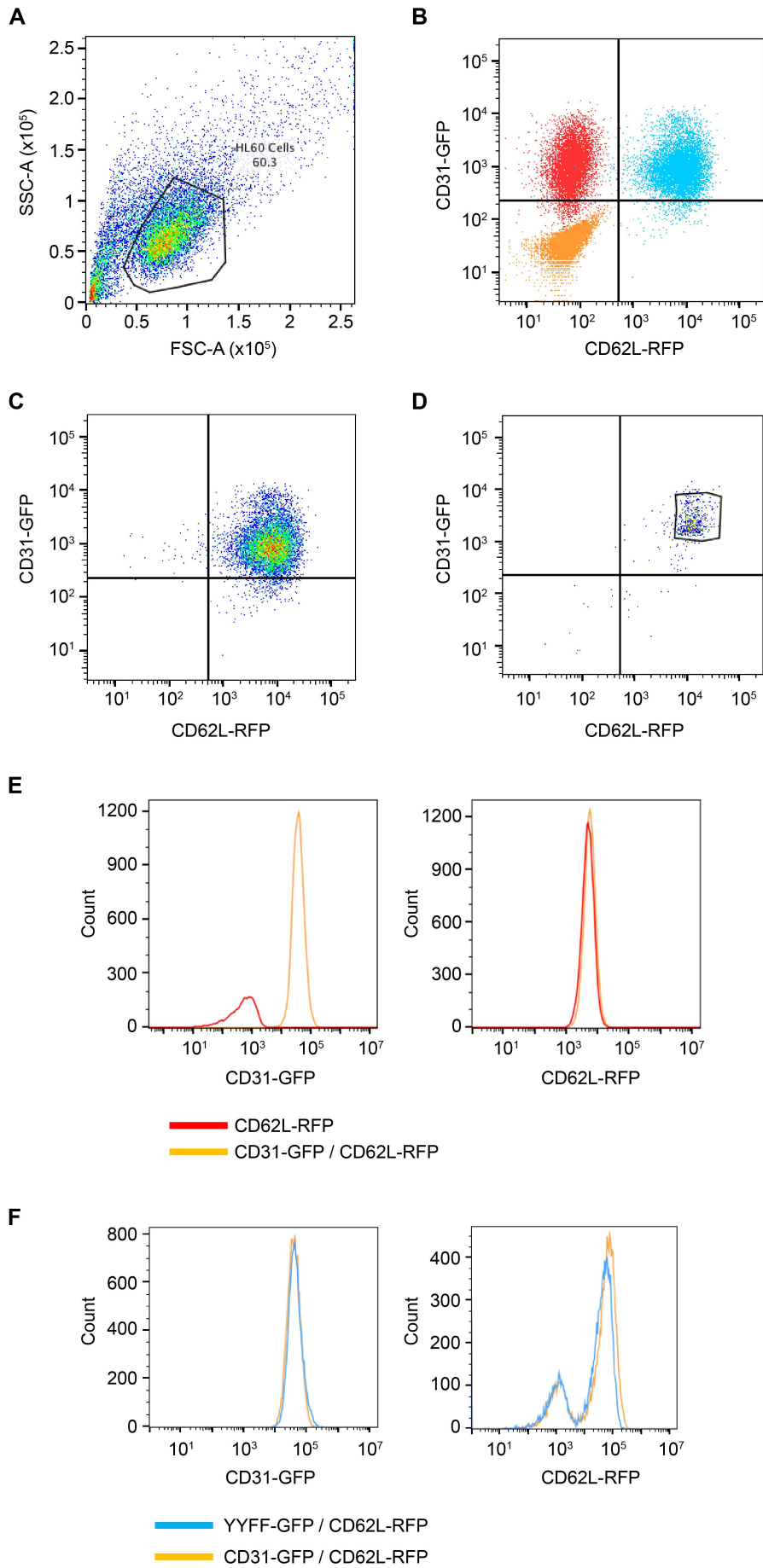
Supplementary Figure 5

Fig. S5

Sorting of HL-60 cells after lentiviral transduction

HL-60 cells stably expressing CXCR2 were transduced with lentiviral particles possessing the open reading frames for PECAM-1-GFP and/or L-selectin-RFP (with a multiplicity of infection (MOI) of 10 for each construct). Cells were subsequently sorted prior to flow assays and FRET/FLIM experiments. (A) Lentivirally transduced cells were gated for the live cell population (black polygon). (B) Another gating event created quadrants based on expression: CD31-GFP$^-$ CD62L-RFP$^-$ (lower left, orange scatter); CD31-GFP$^+$ CD62L-RFP$^-$ (upper left scatter red scatter); CD31-GFP$^+$ CD62L-RFP$^+$ (upper right blue scatter); and CD31-GFP$^-$ CD62L$^+$ (lower right). (C) In an example of sorting for double-expressing cell lines, of the CD31-GFP$^+$ CD62L-RFP$^+$ population of live cells, (D) the top 5% were sorted and isolated from the sample. These cells were then cultured and cryopreserved for use in future assays. (E) FACS histograms provided are examples of similar expression levels between sorted single expressing L-selectin-RFP (red line) and the double expressing PECAM-1-GFP and L-selectin-RFP cell lines. The left histogram represents fluorescence intensity measurements of PECAM-1-GFP and the right histogram shows fluorescence intensity measurements of L-selectin-RFP. (F) Histogram plots of relative expression levels of PECAM-1 (left hand histogram) and L-selectin (right hand histogram) in the double-expressing cell lines: YYFF-PECAM-1-GFP/L-selectin-RFP and PECAM-1-GFP and L-selectin-RFP. It is noteworthy to mention that the FACS profiles of (E) and (F) were acquired on separate occasions.
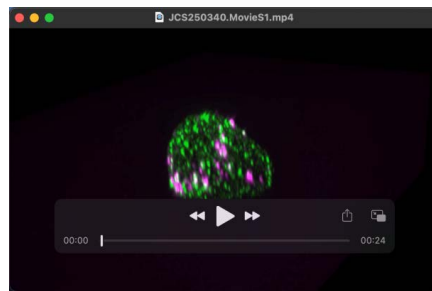
Movie 1
3D reconstituted image of a primary human neutrophil produced from iSIM analysis as described in Figure 1D of the main manuscript. Details of image acquisition are provided in the legend of Figure 1 in the main manuscript and in the Materials and Methods section. Cyan = PECAM-1 clusters. Green = L-selectin. Signal overlap is in white.

Movie 2
Primary human neutrophils were isolated from the whole blood of healthy volunteers and perfused over TNF-α-activated monolayers at a density of 1 x 10^6 cells per mL. The video represents how efficiently neutrophils undergo full TEM in our assays (over 90% efficiency). Phase bright cells are deemed adherent, whereas phase dark cells are deemed fully transmigrated. Time code in red represents minutes, seconds and milliseconds.

Movie 3
A representative video showing a dHL-60 cell undergoing adhesion, crawling and TEM. Stills taken from this movie are provided in Figure 5A of the main manuscript. Time code in red represents minutes, seconds and milliseconds.

Acknowledgements

Authorship contributions

Contribution: I.R. performed experiments, contributed to experimental design, data analysis, statistical analysis, interpretation of findings and writing of the report; A.C.S., J.D., K.R., H.L.H.G. and S.A. performed experiments, contributed to experimental design, data analysis, statistical analysis, interpretation of findings; J.J. contributed to data interpretation and writing of the manuscript; M.J.S & G.C. contributed to experimental design; M.P. performed experiments, contributed to experimental design, data analysis, statistical analysis, interpretation of findings; A.I. conceived the project, contributed to experimental design, data analysis, statistical analysis, interpretation of findings and writing of the report.

Conflict of interest disclosures

There are no conflicts of interest to disclose among any of the authors.

References

Allport, J. R., Ding, H., Collins, T., Gerritsen, M. E. and Luscinskas, F. W. (1997a). Endothelial-dependent mechanisms regulate leukocyte transmigration: a process involving the proteasome and disruption of the vascular endothelial-cadherin complex at endothelial cell-to-cell junctions. *J Exp Med* **186**, 517-27.

Allport, J. R., Ding, H. T., Ager, A., Steeber, D. A., Tedder, T. F. and Luscinskas, F. W. (1997b). L-selectin shedding does not regulate human neutrophil attachment, rolling, or transmigration across human vascular endothelium in vitro. *J Immunol* **158**, 4365-72.

Bjorkman, L., Christenson, K., Davidsson, L., Martensson, J., Amirbeagi, F., Welin, A., Forsman, H., Karlsson, A., Dahlgren, C. and Bylund, J. (2018). Neutrophil recruitment to inflamed joints can occur without cellular priming. *J Leukoc Biol*.

Bradfield, P. F., Scheiermann, C., Nourshargh, S., Ody, C., Luscinskas, F. W., Rainger, G. E., Nash, G. B., Miljkovic-Licina, M., Aurrand-Lions, M. and Imhof, B. A. (2007). JAM-C regulates unidirectional monocyte transendothelial migration in inflammation. *Blood* **110**, 2545-55.

Burns, S. O., Killock, D. J., Moulding, D. A., Metelo, J., Nunes, J., Taylor, R. R., Forge, A., Thrasher, A. J. and Ivetic, A. (2010). A congenital activating mutant of WASp causes altered plasma membrane topography and adhesion under flow in lymphocytes. *Blood* **115**, 5355-65.

Cappenberg, A., Margraf, A., Thomas, K., Bardel, B., McCreedy, D. A., Van Marck, V., Mellmann, A., Lowell, C. A. and Zarbock, A. (2019). L-selectin shedding affects bacterial clearance in the lung: a new regulatory pathway for integrin outside-in signaling. *Blood* **134**, 1445-1457.

Celie, J. W., Beelen, R. H. and van den Born, J. (2009). Heparan sulfate proteoglycans in extravasation: assisting leukocyte guidance. *Front Biosci* **14**, 4932-49.

Chen, A., Engel, P. and Tedder, T. F. (1995). Structural requirements regulate endoproteolytic release of the L-selectin (CD62L) adhesion receptor from the cell surface of leukocytes. *J Exp Med* **182**, 519-30.

Chen, Q., Wang, W. C., Bruce, R., Li, H., Schleider, D. M., Mulbury, M. J., Bain, M. D., Wallace, P. K., Baumann, H. and Evans, S. S. (2004). Central role of IL-6 receptor signal-transducing chain gp130 in activation of L-selectin adhesion by fever-range thermal stress. *Immunity* **20**, 59-70.

Christofidou-Solomidou, M., Nakada, M. T., Williams, J., Muller, W. A. and DeLisser, H. M. (1997). Neutrophil platelet endothelial cell adhesion molecule-1 participates in neutrophil recruitment at inflammatory sites and is down-regulated after leukocyte extravasation. *J Immunol* **158**, 4872-8.

Devilard, E., Xerri, L., Dubreuil, P., Lopez, M. and Reymond, N. (2013). Nectin-3 (CD113) interacts with Nectin-2 (CD112) to promote lymphocyte transendothelial migration. *PLoS One* **8**, e77424.

Evans, S. S., Schleider, D. M., Bowman, L. A., Francis, M. L., Kansas, G. S. and Black, J. D. (1999). Dynamic association of L-selectin with the lymphocyte cytoskeletal matrix. *J Immunol* **162**, 3615-24.

Florey, O., Durgan, J. and Muller, W. (2010). Phosphorylation of leukocyte PECAM and its association with detergent-resistant membranes regulate transendothelial migration. *J Immunol* **185**, 1878-86.

Gamulescu, M. A., Seifert, K., Tingart, M., Falet, H. and Hoffmeister, K. M. (2003). Platelet moesin interacts with PECAM-1 (CD31). *Platelets* **14**, 211-7.

Huang, M. T., Larbi, K. Y., Scheiermann, C., Woodfin, A., Gerwin, N., Haskard, D. O. and Nourshargh, S. (2006). ICAM-2 mediates neutrophil transmigration in vivo: evidence for stimulus specificity and a role in PECAM-1-independent transmigration. *Blood* **107**, 4721-7.

Ivetic, A. (2018). A head-to-tail view of L-selectin and its impact on neutrophil behaviour. *Cell Tissue Res* **371**, 437-453.

Ivetic, A., Deka, J., Ridley, A. and Ager, A. (2002). The cytoplasmic tail of L-selectin interacts with members of the Ezrin-Radixin-Moesin (ERM) family of proteins: cell activation-dependent binding of Moesin but not Ezrin. *J Biol Chem* **277**, 2321-9.

Ivetic, A., Hoskins Green, H. L. and Hart, S. J. (2019). L-selectin: A Major Regulator of Leukocyte Adhesion, Migration and Signaling. *Front Immunol* **10**, 1068.

Kawashima, H., Hirose, M., Hirose, J., Nagakubo, D., Plaas, A. H. and Miyasaka, M. (2000). Binding of a large chondroitin sulfate/dermatan sulfate proteoglycan, versican, to L-selectin, P-selectin, and CD44. *J Biol Chem* **275**, 35448-56.

Kawashima, H., Li, Y. F., Watanabe, N., Hirose, J., Hirose, M. and Miyasaka, M. (1999). Identification and characterization of ligands for L-selectin in the kidney. I. Versican, a large chondroitin sulfate proteoglycan, is a ligand for L-selectin. *Int Immunol* **11**, 393-405.

Killock, D. J. and Ivetic, A. (2010). The cytoplasmic domains of TNFalpha-converting enzyme (TACE/ADAM17) and L-selectin are regulated differently by p38 MAPK and PKC to promote ectodomain shedding. *Biochem J* **428**, 293-304.

Kitaya, K. and Yasuo, T. (2009). Dermatan sulfate proteoglycan biglycan as a potential selectin L/CD44 ligand involved in selective recruitment of peripheral blood CD16(-) natural killer cells into human endometrium. *J Leukoc Biol* **85**, 391-400.

Ley, K., Hoffman, H. M., Kubes, P., Cassatella, M. A., Zychlinsky, A., Hedrick, C. C. and Catz, S. D. (2018). Neutrophils: New insights and open questions. *Sci Immunol* **3**.

Ley, K., Laudanna, C., Cybulsky, M. I. and Nourshargh, S. (2007). Getting to the site of inflammation: the leukocyte adhesion cascade updated. *Nat Rev Immunol* **7**, 678-89.

Li, X., Steeber, D. A., Tang, M. L., Farrar, M. A., Perlmutter, R. M. and Tedder, T. F. (1998). Regulation of L-selectin-mediated rolling through receptor dimerization. *J Exp Med* **188**, 1385-90.

Lou, O., Alcaide, P., Luscinskas, F. W. and Muller, W. A. (2007). CD99 is a key mediator of the transendothelial migration of neutrophils. *J Immunol* **178**, 1136-43.

Ludwig, R. J., Zollner, T. M., Santoso, S., Hardt, K., Gille, J., Baatz, H., Johann, P. S., Pfeffer, J., Radeke, H. H., Schon, M. P. et al. (2005). Junctional adhesion molecules (JAM)-B and -C contribute to leukocyte extravasation to the skin and mediate cutaneous inflammation. *J Invest Dermatol* **125**, 969-76.

Morikis, V. A., Chase, S., Wun, T., Chaikof, E. L., Magnani, J. L. and Simon, S. I. (2017). Selectin catch-bonds mechanotransduce integrin activation and neutrophil arrest on inflamed endothelium under shear flow. *Blood*.

Muller, W. A. (2011). Mechanisms of leukocyte transendothelial migration. *Annu Rev Pathol* **6**, 323-44.

Muller, W. A., Weigl, S. A., Deng, X. and Phillips, D. M. (1993). PECAM-1 is required for transendothelial migration of leukocytes. *J Exp Med* **178**, 449-60.

Newe, A., Rzeniewicz, K., Konig, M., Schroer, C. F. E., Joachim, J., Rey-Gallardo, A., Marrink, S. J., Deka, J., Parsons, M. and Ivetic, A. (2019). Serine Phosphorylation of L-Selectin Regulates ERM Binding, Clustering, and Monocyte Protrusion in Transendothelial Migration. *Front Immunol* **10**, 2227.

Paddock, C., Zhou, D., Lertkiatmongkol, P., Newman, P. J. and Zhu, J. (2016). Structural basis for PECAM-1 homophilic binding. *Blood* **127**, 1052-61.

Palecanda, A., Walcheck, B., Bishop, D. K. and Jutila, M. A. (1992). Rapid activation-independent shedding of leukocyte L-selectin induced by cross-linking of the surface antigen. *Eur J Immunol* **22**, 1279-86.

Parsons, M., Messent, A. J., Humphries, J. D., Deakin, N. O. and Humphries, M. J. (2008). Quantification of integrin receptor agonism by fluorescence lifetime imaging. *J Cell Sci* **121**, 265-71.

Pellegatta, F., Chierchia, S. L. and Zocchi, M. R. (1998). Functional association of platelet endothelial cell adhesion molecule-1 and phosphoinositide 3-kinase in human neutrophils. *J Biol Chem* **273**, 27768-71.

Phong, M. C., Gutwein, P., Kadel, S., Hexel, K., Altevogt, P., Linderkamp, O. and Brenner, B. (2003). Molecular mechanisms of L-selectin-induced co-localization in rafts and shedding [corrected]. *Biochem Biophys Res Commun* **300**, 563-9.

Privratsky, J. R., Paddock, C. M., Florey, O., Newman, D. K., Muller, W. A. and Newman, P. J. (2011). Relative contribution of PECAM-1 adhesion and signaling to the maintenance of vascular integrity. *J Cell Sci* **124**, 1477-85.

Pruenster, M., Kurz, A. R., Chung, K. J., Cao-Ehlker, X., Bieber, S., Nussbaum, C. F., Bierschenk, S., Eggersmann, T. K., Rohwedder, I., Heinig, K. et al. (2015). Extracellular MRP8/14 is a regulator of beta2 integrin-dependent neutrophil slow rolling and adhesion. *Nat Commun* **6**, 6915.

Reijerkerk, A., Kooij, G., van der Pol, S. M., Khazen, S., Dijkstra, C. D. and de Vries, H. E. (2006). Diapedesis of monocytes is associated with MMP-mediated occludin disappearance in brain endothelial cells. *FASEB J* **20**, 2550-2.

Rey-Gallardo, A., Tomlins, H., Joachim, J., Rahman, I., Kitscha, P., Frudd, K., Parsons, M. and Ivetic, A. (2018). Sequential binding of ezrin and moesin to L-selectin regulates monocyte protrusive behaviour during transendothelial migration. *J Cell Sci* **131**.

Rzeniewicz, K., Newe, A., Rey Gallardo, A., Davies, J., Holt, M. R., Patel, A., Charras, G. T., Stramer, B., Molenaar, C., Tedder, T. F. et al. (2015). L-selectin shedding is activated specifically within transmigrating pseudopods of monocytes to regulate cell polarity in vitro. *Proc Natl Acad Sci U S A* **112**, E1461-70.

Sai, J., Walker, G., Wikswo, J. and Richmond, A. (2006). The IL sequence in the LLKIL motif in CXCR2 is required for full ligand-induced activation of Erk, Akt, and chemotaxis in HL60 cells. *J Biol Chem* **281**, 35931-41.

Schenkel, A. R., Chew, T. W., Chlipala, E., Harbord, M. W. and Muller, W. A. (2006). Different susceptibilities of PECAM-deficient mouse strains to spontaneous idiopathic pneumonitis. *Exp Mol Pathol* **81**, 23-30.

Smith, C. W., Kishimoto, T. K., Abbassi, O., Hughes, B., Rothlein, R., McIntire, L. V., Butcher, E. and Anderson, D. C. (1991). Chemotactic factors regulate lectin adhesion molecule 1 (LECAM-1)-dependent neutrophil adhesion to cytokine-stimulated endothelial cells in vitro. *J Clin Invest* **87**, 609-18.

Smolen, J. E., Petersen, T. K., Koch, C., O'Keefe, S. J., Hanlon, W. A., Seo, S., Pearson, D., Fossett, M. C. and Simon, S. I. (2000). L-selectin signaling of neutrophil adhesion and degranulation involves p38 mitogen-activated protein kinase. *J Biol Chem* **275**, 15876-84.

Spertini, O., Kansas, G. S., Reimann, K. A., Mackay, C. R. and Tedder, T. F. (1991). Function and evolutionary conservation of distinct epitopes on the leukocyte adhesion molecule-1 (TQ-1, Leu-8) that regulate leukocyte migration. *J Immunol* **147**, 942-9.

Stadtmann, A., Germena, G., Block, H., Boras, M., Rossaint, J., Sundd, P., Lefort, C., Fisher, C. I., Buscher, K., Gelschefarth, B. et al. (2013). The PSGL-1-L-selectin signaling complex regulates neutrophil adhesion under flow. *J Exp Med* **210**, 2171-80.

Stoler-Barak, L., Moussion, C., Shezen, E., Hatzav, M., Sixt, M. and Alon, R. (2014). Blood vessels pattern heparan sulfate gradients between their apical and basolateral aspects. *PLoS One* **9**, e85699.

Thompson, R. D., Noble, K. E., Larbi, K. Y., Dewar, A., Duncan, G. S., Mak, T. W. and Nourshargh, S. (2001). Platelet-endothelial cell adhesion molecule-1 (PECAM-1)-deficient mice demonstrate a transient and cytokine-specific role for PECAM-1 in leukocyte migration through the perivascular basement membrane. *Blood* **97**, 1854-60.

Venturi, G. M., Tu, L., Kadono, T., Khan, A. I., Fujimoto, Y., Oshel, P., Bock, C. B., Miller, A. S., Albrecht, R. M., Kubes, P. et al. (2003). Leukocyte migration is regulated by L-selectin endoproteolytic release. *Immunity* **19**, 713-24.

Wang, W. C., Goldman, L. M., Schleider, D. M., Appenheimer, M. M., Subjeck, J. R., Repasky, E. A. and Evans, S. S. (1998). Fever-range hyperthermia enhances L-selectin-dependent adhesion of lymphocytes to vascular endothelium. *J Immunol* **160**, 961-9.

Woodfin, A., Voisin, M. B., Beyrau, M., Colom, B., Caille, D., Diapouli, F. M., Nash, G. B., Chavakis, T., Albelda, S. M., Rainger, G. E. et al. (2011). The junctional adhesion molecule JAM-C regulates polarized transendothelial migration of neutrophils in vivo. *Nat Immunol* **12**, 761-9.

Woodfin, A., Voisin, M. B., Imhof, B. A., Dejana, E., Engelhardt, B. and Nourshargh, S. (2009). Endothelial cell activation leads to neutrophil transmigration as supported by the sequential roles of ICAM-2, JAM-A, and PECAM-1. *Blood* **113**, 6246-57.

Yadav, S. K., Feigelson, S. W., Roncato, F., Antman-Passig, M., Shefi, O., Lammerding, J. and Alon, R. (2018). Frontline Science: Elevated nuclear lamin A is permissive for granulocyte transendothelial migration but not for motility through collagen I barriers. *J Leukoc Biol* **104**, 239-251.
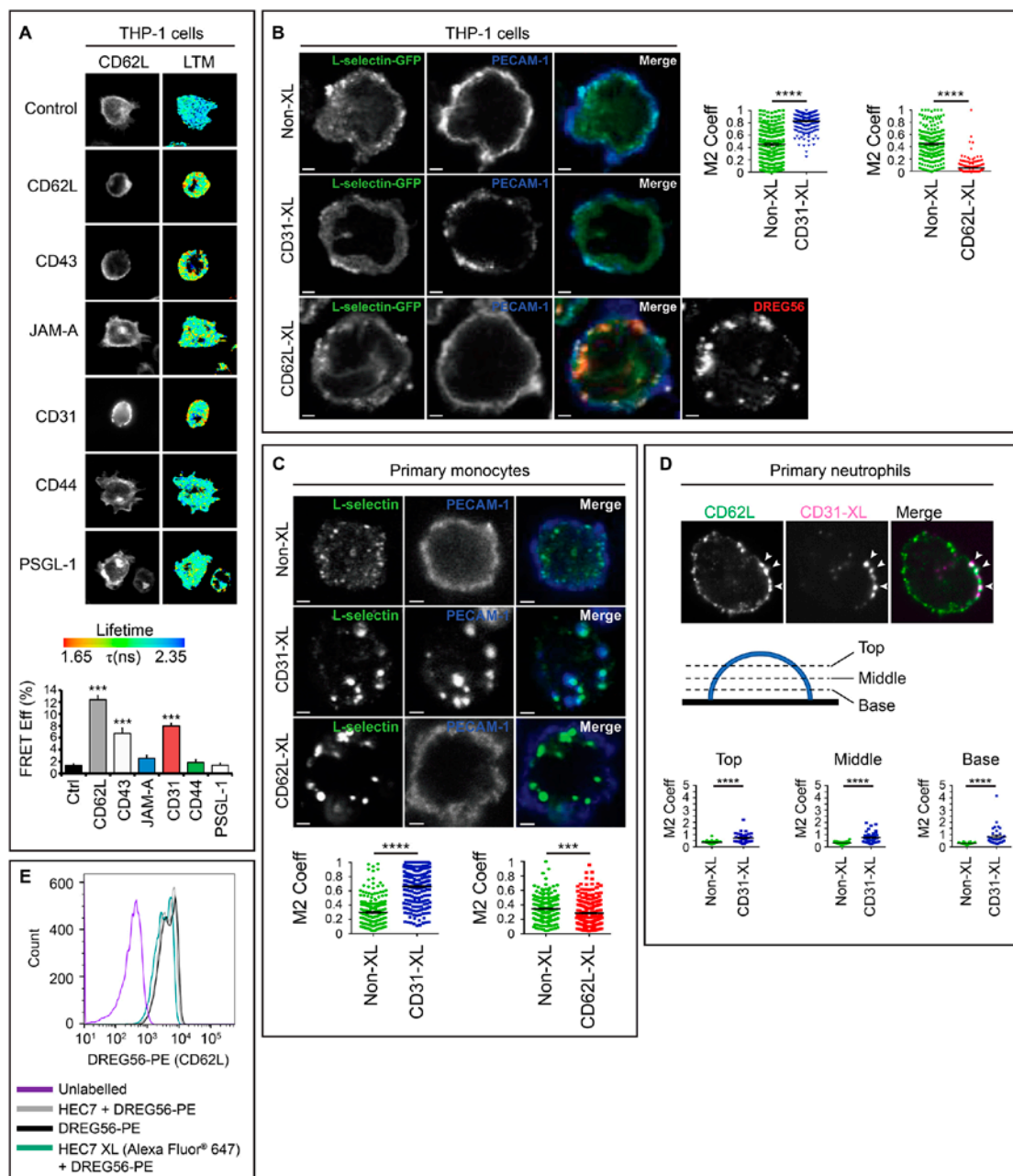
Figures

Figure 1
Antibody-mediated clustering of PECAM-1 drives inside-out clustering of L-selectin and its co-clustering with PECAM-1
(A) THP-1 cells expressing L-selectin-GFP/RFP were treated with a range of primary antibodies targeting L-selectin (CD62L), CD43, JAM-A, PECAM-1 (CD31), CD44 or PSGL-1. Primary antibodies were subsequently clustered with secondary antibody and cells plated onto poly-L-lysine (PLL), fixed in 4% PFA and prepared for FRET/FLIM analysis. GFP fluorescence channel and lifetime (LTM) images are provided for each cell line. The lifetime of fluorescence is expressed in a pseudocolour scale from red (low lifetime with a very high probability of interaction) to blue (high lifetime with a very low probability of interaction). Bar graph represents data acquired from at least 45 cells across 3 independent

experiments. Error bars represent S.E.M. Statistical analysis: One-way ANOVA followed by Tukey's post-test. ***=p<0.001. (B) Confocal microscopy was used to monitor the effect of clustering either PECAM-1 (CD31-XL) or L-selectin-GFP (CD62L) on THP-1 cells. At least 200 cells were analysed. Manders' Overlap Coefficient (M2 Coeff) was used to quantify the extent of overlap between signals corresponding to CD31 and CD62L, represented in the column scatter graph. Two-tailed unpaired student's T-test with Welch's correction used. **** = P < 0.0001. Mean ± SEM. Scale bar = 2.5 μm. (C) Primary human CD14-positive monocytes were purified from healthy donor bloods and clustering of either CD31 or CD62L were performed as described in (B). M2 Coeff was used as a measure of colocalisation between signals corresponding to CD31 and CD62L, represented in the column scatter graph. At least 200 cells were analysed per treatment across at least three independent experiments. Two-tailed unpaired student's T-test with Welch's correction used. *** = P < 0.001, **** = P < 0.0001. Mean ± SEM. Scale bar = 2.5 μm. (D) iSIM was used to monitor the impact of clustering CD31 on the co-clustering behaviour of CD62L in primary human neutrophils. Cells were left untreated (Non-XL) or antibodies used to cluster CD31 (CD31-XL) as in (B). Cells were plated onto poly-L-lysine and incubated at 37ºC before fixation in 4% PFA. LAM1-14 monoclonal antibody was used to stain endogenous L-selectin, followed by donkey anti-mouse secondary antibody conjugated to Alexa Fluor® 488. Representative iSIM cross-sectional view of a neutrophil clustered with primary anti-CD31 antibody and secondary donkey anti-sheep antibody conjugated to Alexa Fluor® 633. Three different optical sections were taken, as depicted in the cartoon, and Mander's overlap co-efficient (M2 Coeff) was used to quantify the extent of overlap between the two signals. Averages are derived from 38 cells for each treatment across three independent experiments. Two-tailed unpaired student's T-test with Welch's correction used. **** = P < 0.0001. Mean ± SEM. (E) Flow cytometric analysis of primary human neutrophils treated with the anti-PECAM-1 monoclonal antibody, HEC7. Neutrophils were treated with HEC7 alone (grey line) or HEC7 plus a secondary clustering antibody conjugated to Alexa Fluor® 647 (green line). DREG56 directly conjugated to phycoerythrin (PE) was used to monitor L-selectin expression in untreated cells (black line), and cells with HEC7 alone (grey line) or with HEC7 plus clustering secondary antibody (green line). Purple line represents unstained neutrophils. Histogram is representative of three independent experiments (see Fig. S1 & S2).
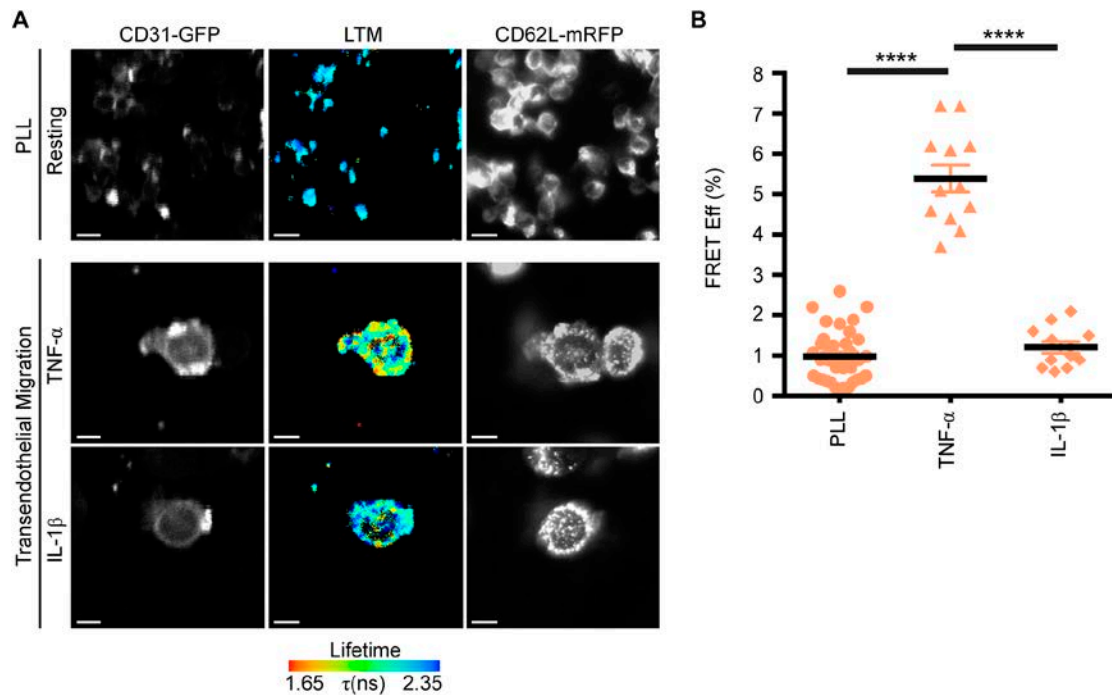
Figure 2

Co-clustering of L-selectin with PECAM-1 occurs exclusively during TEM in a cytokine-specific manner

(A) dHL-60 cells co-expressing L-selectin-RFP and PECAM-1-GFP were plated onto poly-L-lysine (PLL) at 37°C for 5 min and then rapidly fixed in 4% PFA. FLIM was used to monitor the FRET efficiency between the GFP and RFP tags. (B) Differentiated HL-60 cells co-expressing PECAM-1-GFP and L-selectin-RFP were perfused over TNF-α-, or IL-1β-, activated HUVEC. Cells were rapidly fixed in 4% PFA when the majority of cells were observed undergoing mid-TEM. Given that endothelial PECAM-1 is enriched at cell-to-cell junctions, FLIM/FRET measurements were acquired in dHL-60 cells captured in mid-TEM (i.e. within regions that were neither exclusively above nor below the endothelium). Panels display the green channel for PECAM-1-GFP (left column), the GFP lifetime (middle column, LTM) and the red channel for L-selectin-RFP (right column). The fluorescence lifetime of GFP is provided as a pseudocolour scale of blue (long lifetime = little to no FRET) to red (short lifetime = FRET). Quantification of FRET efficiency between PECAM-1-GFP and L-selectin-RFP was acquired through an average measurement from 35 cells analysed under resting conditions and from 12 cells caught in mid-transmigration across either TNF-α- or IL1-β-activated HUVEC. Measurements are derived from three independent experiments. One-way ANOVA followed by multiple comparisons corrected for by the Sidak method. **** = P < 0.0001. Mean ± SEM. Scale bar = 5 μm.
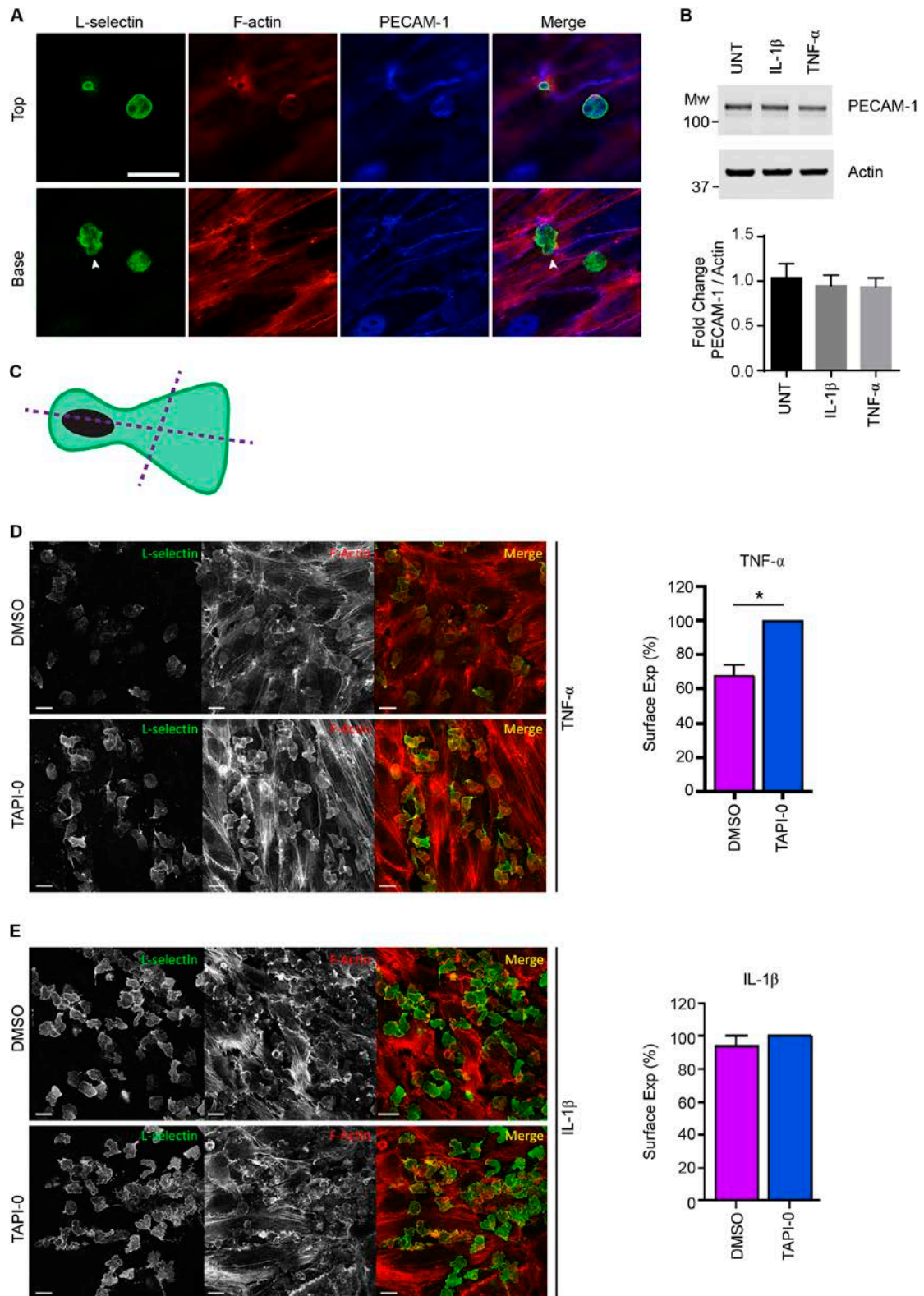
Figure 3

L-selectin shedding is activated in neutrophils crossing TNF-α-, but not IL-1β-, activated HUVEC.

(A) Primary human neutrophils were perfused over TNF-α-activated HUVEC monolayers and after 6 min of perfusion were fixed in 4% paraformaldehyde and prepared for immunostaining for PECAM-1 (blue – Alexa Fluor® 633), L-selectin

(green - Alexa Fluor® 488) and F-actin (red – TRITC phalloidin). Two primary human neutrophils are captured in different stages of the multi-step adhesion cascade: firm adhesion (right hand side) and mid-TEM (left-hand side) under flow conditions. Two optical sections, Top and Base, reveal the subcellular organisation of endogenous L-selectin present within the transmigrated pseudopod (arrowhead) and the non-transmigrated cell body (or uropod). Distinct morphological characteristics of flat pseudopodial extensions in the subendothelial space and rounded non-transmigrated body afford easy interpretation of transmigrated and non-transmigrated regions. Anti-PECAM-1 staining of TNF-α-activated HUVEC reveals the well-documented discontinuity of the signal specifically at the region of paracellular TEM. Note that L-selectin expression is present in both the transmigrated pseudopod and non-transmigrated uropod, which is has been observed in primary human (CD14-positive) monocytes (Rzeniewicz et al., 2015) (B) Analysis of HUVEC PECAM-1 protein expression through Western blot analysis, following overnight stimulation with or without the cytokines IL-1β and TNF-α (UNT = untreated). Anti-actin Western blot is used as a loading control for PECAM-1. Bar graph represents the average band intensity values corresponding to PECAM-1, after normalisation against the actin Western blot bands (n = 3 independent experiments). (C) Schematic representation of how line intensity profiles were drawn and quantified for neutrophils within the subendothelial space. More details are provided in the Materials and Methods section. (D) Primary human neutrophils, pre-treated for 20 min with either DMSO or 10 μM TAPI-0, were perfused over TNF-α-activated HUVEC monolayers at a density of 1×10^6 cells per mL. Cells were perfused for 5 min, followed by a further 15 min with neat HL-60 media. By the end of perfusion, over 95% of all neutrophils had successfully completed TEM (see Movie 2). Specimens were immediately fixed in 4% PFA prior to premeabilisation and immunostaining for L-selectin with LAM1-14 and TRITC-phalloidin. Bar graph showing L-selectin surface expression, quantified as a percentage of the LAM1-14 signal that is relative to the maximal L-selectin signal assigned to the fluorescence intensity in the TAPI-0 treatment group (set at 100%). At least 420 cells were analysed per group across three independent experiments. Two-tailed unpaired student's T-test with Welch's correction was used. * = P < 0.05. Mean ± SEM. Scale bar = 10 μm. (E) Primary human neutrophils were perfused over IL-1β-activated HUVEC using the same method as in (D). Fluorescence intensity of the LAM1-14 signal corresponding to L-selectin was assessed through analysing line intensity profiles using Volocity software (see (C) and materials and methods). Bar graph showing L-selectin surface expression, quantified as a percentage of the LAM1-14 signal that is relative to the maximal L-selectin signal assigned to the fluorescence intensity in the TAPI-0 treatment group (set at 100%). At least 420 cells were analysed per group across three independent experiments. Two-tailed unpaired student's T-test with Welch's correction used. Mean ± SEM. Scale bar = 10 μm.
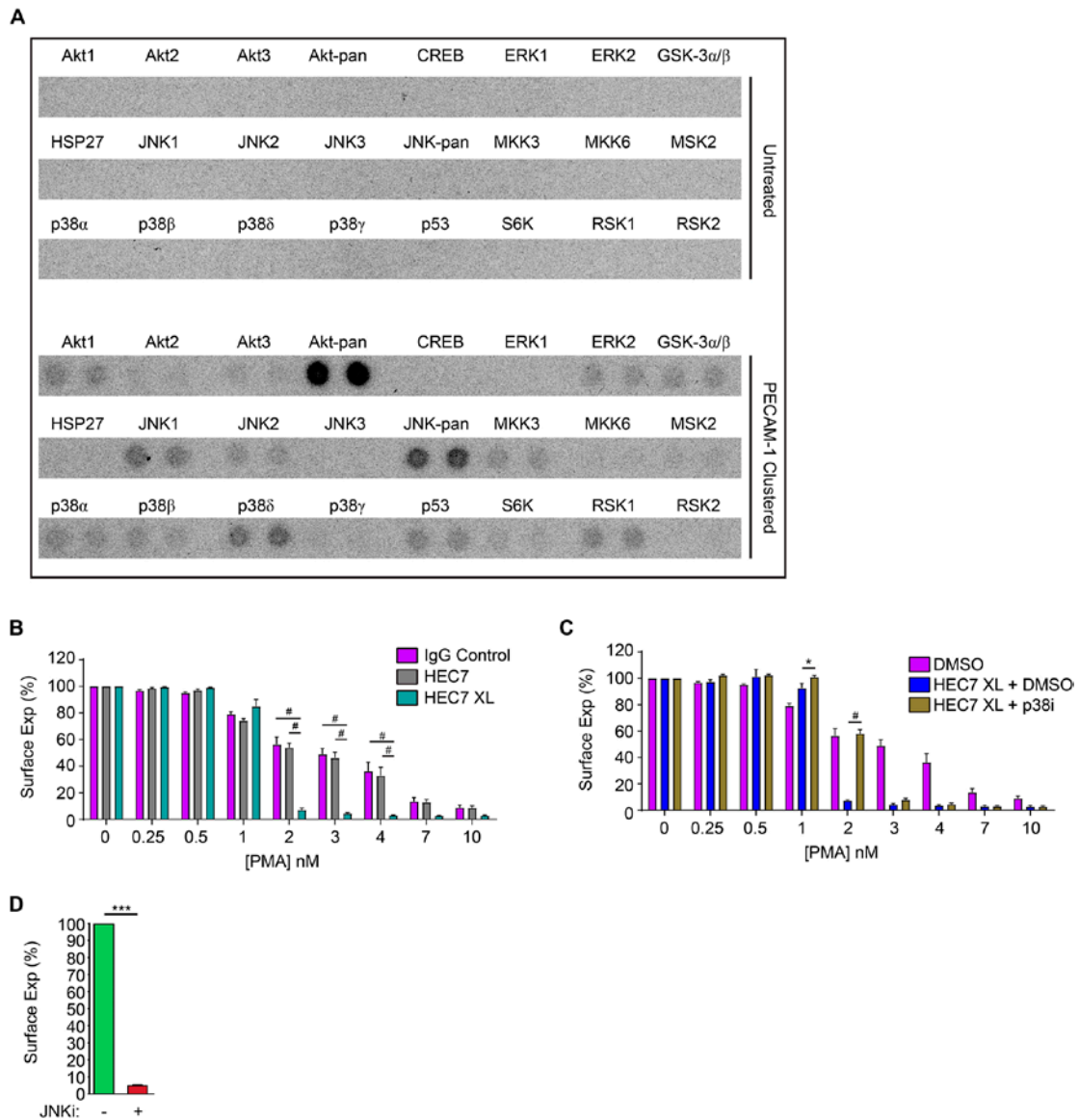
Figure 4

Clustering neutrophil PECAM-1 activates Akt, MAP kinases, and potentiates ectodomain shedding of L-selectin. (A) MAPK array (R&D Systems) of primary human neutrophils clustered with HEC7 and of secondary antibody. Upper panel represents untreated cells and lower panel is PECAM-1-clustered cells. See Materials and Methods section for more detail. (B) Control Neutrophils isolated from healthy volunteers were labelled with either control IgG (purple bars), HEC7 (grey bars) or HEC7 plus clustering secondary antibody (turquoise bars). All labelling procedures were performed in the presence of Fc receptor block to avoid any non-specific binding and clustering of neutrophil Fc receptors (see materials and methods for more details). Antibody-labelled neutrophils were subsequently challenged with an increasing range of PMA concentrations (0.25 – 10 nM) and incubated for 30 min at 37ºC. Alexa Fluor® 647-conjugated DREG56 monoclonal antibody was used to monitor L-selectin expression by flow cytometry. Fluorescence values were compared against untreated cells, which in turn were normalised to a value of 100%. Bar graph is representative of three independent experiments using three different donors. # = P < 0.0001. Mean ± SEM. (C)

Neutrophils isolated from healthy donors were subjected to IgG control (purple bars) and HEC7 labelling as in (B). Prior to and during the secondary antibody labelling procedure, which cross-links PECAM-1 on neutrophils, cells were concomitantly incubated with either DMSO (carrier control) (blue bars) or 25 μM of the p38 MAPK inhibitor, SB202190 (p38i, gold bars) at 37°C. Cells were then subjected, as in (B), to increasing doses of PMA at 30°C for 30 min and Alexa Fluor® 647-conjugated DREG56 monoclonal antibody was used to monitor L-selectin expression by flow cytometry. Fluorescence values were compared against untreated cells, which in turn were normalised to 100%. Bar graph is representative of 10,000 events, each collected over three independent experiments using three different donors. * = P < 0.05; # = P < 0.0001. Mean ± SEM. (D) Neutrophils were incubated with either DMSO carrier (green bar) or 50 μM of the JNK inhibitor SP600125 (JNKi, red bar) for 30 min at 37°C. L-selectin levels were subsequently quantified by flow cytometry. Data represents the mean ±SEM of at least 3 independent experiments and all data were collected in triplicate. Statistical significance was calculated by unpaired student's T-test. p *** <0.001.
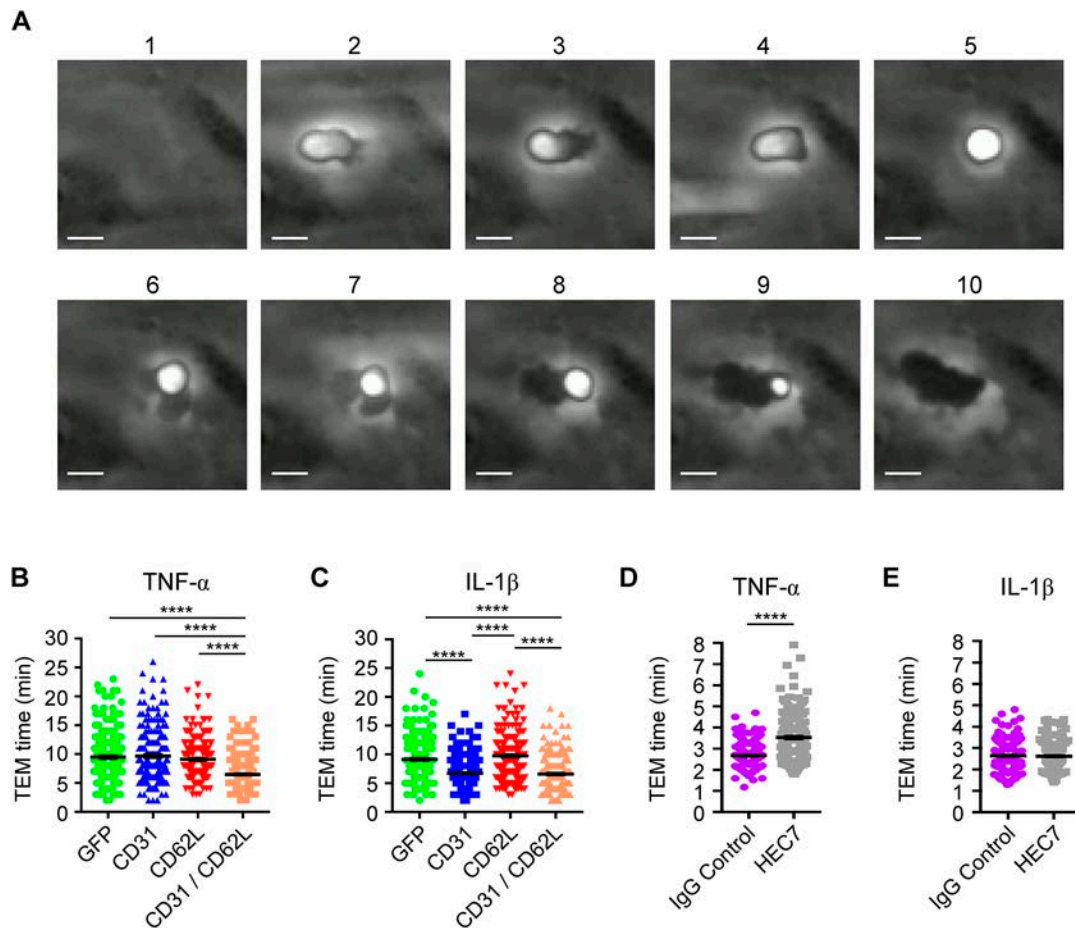
Figure 5

Co-expression of L-selectin and PECAM-1 in dHL-60 cells significantly increases TTT across TNF-α-activated HUVEC, and functionally blocking PECAM-1 in primary human neutrophils significantly reduces TTT across TNF-α-activated HUVEC

(A) Time series of frames (from Movie 3, which includes the time code) showing how TEM of HL-60 cells is quantified. Cells transitioning from phase bright (image 2) to completely phase dark (image 10). Scale bar = 5 μm. (B) Quantification of average TTT for dHL-60 cells transmigrating across TNF-α-activated HUVEC. The dHL-60 cells analysed are stably expressing: GFP alone (green column scatter), PECAM-1-GFP alone (blue column scatter), L-selectin-RFP alone (red column scatter), or fluorescently tagged constructs of both PECAM-1 and L-selectin (orange column scatter). The TTT of at least 180 cells were quantified per group across three independent experiments. One-way ANOVA followed by multiple comparisons corrected for by the Sidak method. **** = P < 0.0001. Mean ± SEM. (C) Quantification of average TTT for dHL-60 cells transmigrating across IL-1β-activated HUVEC. The dHL-60 cells analysed are stably expressing: GFP alone (green column scatter), PECAM-1-GFP alone (blue column scatter), L-selectin-RFP alone (red column scatter), or fluorescently tagged constructs of both PECAM-1 and L-selectin (orange column scatter). The TTT of at least 180 cells were quantified per group across three independent experiments. One-way ANOVA followed by multiple comparisons corrected for by the Sidak method. **** = P < 0.0001. Mean ± SEM. (D) Primary human neutrophils were pre-treated with either

1 µg/mL anti-PECAM-1 function-blocking antibody (HEC7) or isotype-matched control IgG2a (IgG Control) at 37°C for at least 20 min prior to perfusion over TNF-α-activated HUVEC. TTT were recorded using widefield timelapse microscopy. Column scatter graph represents the average TTT of 140 and 145 cells for IgG2a and HEC7 treatment groups, respectively. Data is collected over three independent experiments using three different donors. Two-tailed unpaired student's T-test with Welch's correction. **** = P < 0.0001.

(E) Primary human neutrophils were pre-treated with either 1 µg/mL anti-PECAM-1 function-blocking antibody (HEC7) or isotype-matched control IgG2a (IgG Control) at 37°C for at least 20 min prior to perfusion over IL-1β-activated HUVEC. TTT were recorded using widefield timelapse microscopy. Column scatter graph represents the average TTT of 140 and 145 cells for IgG2a and HEC7 treatment groups, respectively. Data is collected over three independent experiments using three different donors.
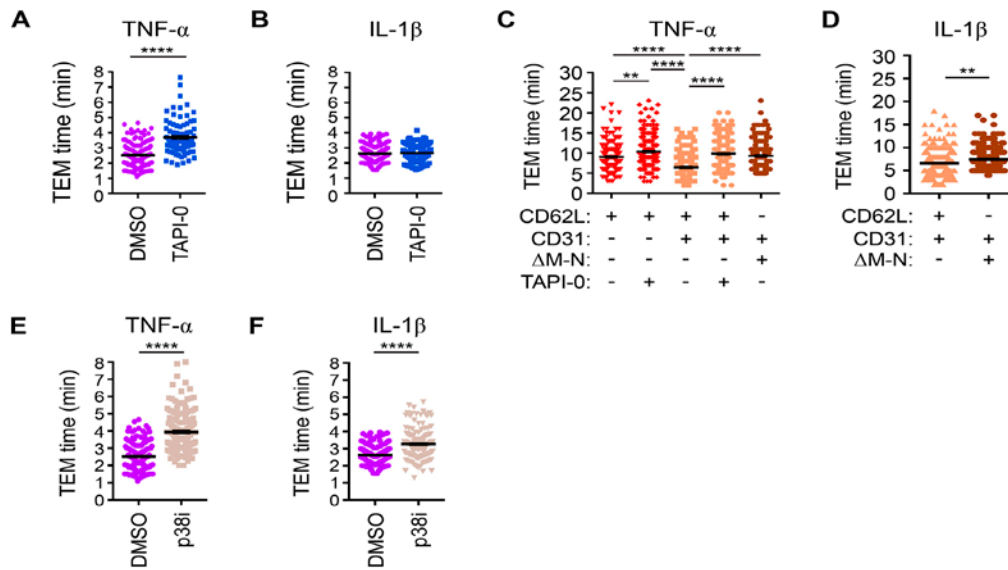
Figure 6

Blocking L-selectin shedding in neutrophils and dHL-60 cells significantly delays TTT across TNF-α-, but not IL-1β-, activated HUVEC monolayers

Primary human neutrophils were pre-treated either with carrier (DMSO) or 10 μM TAPI-0 at 37°C for 20 min prior to perfusion over (A) TNF-a- or (B) IL-1-b- activated HUVEC. Note that in all experiments, either carrier or inhibitor was supplemented into the perfusate. The TTT of neutrophils crossing TNF-a- activated endothelial monolayers was derived from 150 and 90 cells for DMSO and TAPI-0 treatment, respectively. The average time taken for IL1-b-dependent TEM was derived from 150 cells crossing either DMSO or TAPI-0-treatment groups. All measurements were derived from three independent experiments. Two-tailed unpaired student's T-test with Welch's correction used. **** = P < 0.0001. Mean ± SEM. (C) dHL-60 cells stably expressing L-selectin-RFP alone or with PECAM-1- GFP were perfused over TNF-a-activated HUVEC in the absence or presence of 10 μM TAPI-0. The TTT of HL-60 cells were quantified as in Fig. 5B. Column scatter graph in (C) is the average measurement from 180 cells per group and derived from three independent experiments. Note that the scatter plots for CD62L (red) and CD31/CD62L (orange) are reproduced from Fig. 5B for relative comparison. One-way ANOVA followed by multiple comparisons corrected for by the Sidak method. **** = P < 0.0001. Mean ± SEM. (D) dHL-60 cells stably expressing PECAM-1-GFP with either WT L-selectin-RFP or DM-N L-selectin-RFP were perfused under conditions described in Fig. 5C and specifically over IL1-b- activated HUVEC. An average measurement from 180 cells was obtained per group and derived from three independent experiments. Note that the scatter plot for CD31/CD62L (orange) double-expressing cell line is reproduced here from Fig. 5C for relative comparison. Two-tailed unpaired student's T-test with Welch's correction used. ** = P < 0.01. Mean ± SEM. (E&F) Primary human neutrophils were preincubated with 25 mM of the p38 MAPK inhibitor, SB202190, at 37°C for 20 min prior to perfusion over either TNF-a- or IL-1-b-activated HUVEC. Note that the same concentration of the inhibitor was supplemented into the perfusate during the flow assay. TTT were calculated for neutrophils crossing TNF-a- (E) or IL-1-b- (F) activated HUVEC and compared with DMSO control groups from (A) and (B).
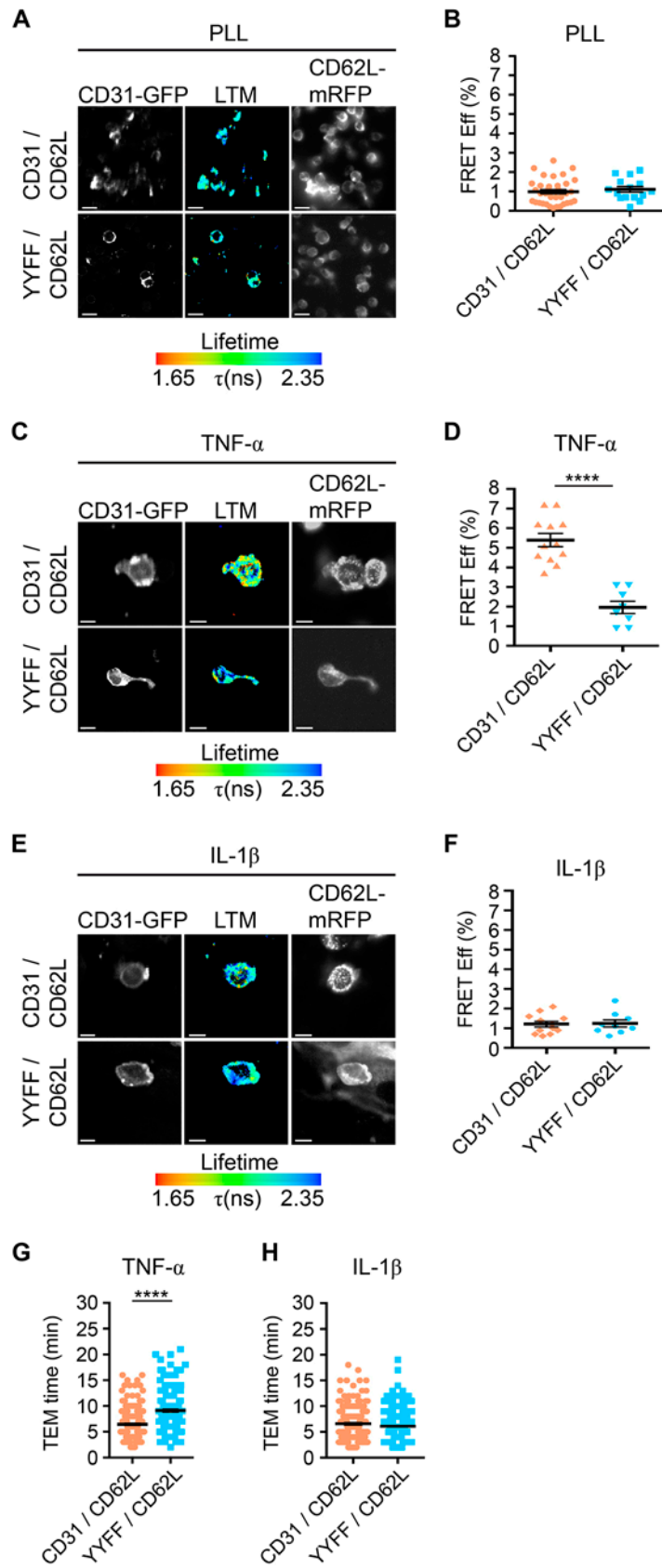
Figure 7

Mutation of Y663 and Y686 within the PECAM-1 ITIM disrupts co-clustering of L-selectin during TEM and retards TTT across TNF-α-activated HUVEC monolayers

(A) As in Fig. 2, HL-60 cells expressing L-selectin-RFP and either WT PECAM-1-GFP or the YYFF PECAM-1-GFP ITIM mutant were seeded onto PLL-coated coverslips and subsequently prepared for FLIM. GFP lifetime (LTM) is provided as a pseudocolour scale of blue (long lifetime) to red (short lifetime). The FRET efficiency was quantified and expressed as a percentage, shown in the column scatter graph (B). (C-F) dHL-60 cells expressing L-selectin-RFP with either WT PECAM-1-GFP or YYFF PECAM-1-GFP were perfused over either TNF-α- or IL-1β-activated HUVEC monolayers as previously described in Fig. 2. Following perfusion, cells were fixed and prepared for FLIM analysis for TNF-α (C&D) or IL-1β (E&F). GFP lifetime (LTM) is provided as a pseudocolour scale of blue (long lifetime) to red (short lifetime). Column scatter graphs contain the average measurement from 180 cells per group and derived from three independent experiments. One-way ANOVA followed by multiple comparisons corrected for by the Sidak method. **** = P < 0.0001. Mean ± SEM. Note that the data and images representing dHL-60 cells stably expressing WT L-selectin and WT PECAM-1 in (A) – (H) are taken from previous analyses (specifically from Figs 2 and 5) to compare against the TEM times for YYFF PECAM-1 and WT L-selectin-expressing cells. Scale bar = 10 μm. (G&H) The same cell lines were perfused over either TNF-α- or IL-1β-activated HUVEC monolayers and TTT was quantified across these monolayers and expressed in the column scatter graphs (G) and (H). Average measurements from 180 cells were obtained per group and derived from three independent experiments. Two-tailed unpaired student's T-test with Welch's correction used. **** = P < 0.0001. Mean ± SEM.

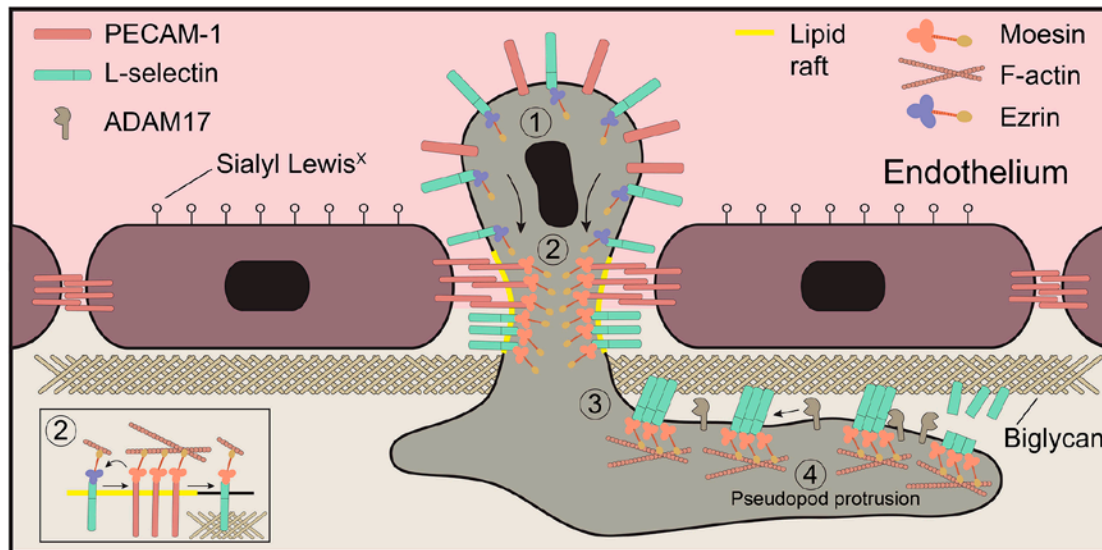**Figure 8**
Working model of L-selectin co-clustering with PECAM-1 during TEM
Schematic of a neutrophil captured in mid-TEM, depicting the molecular events we hypothesise occurs during TEM across TNF-α-activated endothelial monolayers. (1) L-selectin and PECAM-1 remain unclustered in non-transmigrated uropods. (2) Neutrophil PECAM-1 is clustered in *cis* by endothelial PECAM-1 through homotypic interactions via immunoglobulin domains 1 and 2, which drives the co-clustering of L-selectin. (3) We believe that the clustered L-selectin within the subendothelial space could increase its ability to bind subendothelial glycans, such as biglycan, which could drive one of two signals – (4) activation of the sheddase ADAM17 to drive the cleavage of L-selectin (e.g. through activation of p38 MAPK (Smolen et al., 2000)) and (5) signalling downstream of the clustered L-selectin to drive pseudopod protrusion. We have recently shown that ezrin and moesin bind to L-selectin in a sequential manner: ezrin to drive signalling through putative interaction with the p85 regulatory subunit of PI3K (not shown here but reviewed elsewhere (Ivetic et al., 2019)) and moesin to facilitate ectodomain shedding. Ectodomain shedding of L-selectin would limit the extent to which leukocytes drive pseudopod protrusion in the subendothelial space, allowing other mechanisms to successfully establish front-back polarity for interstitial chemotaxis.